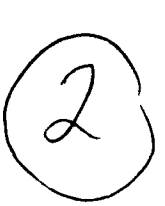

OFFICE OF NAVAL RESEARCH

Grant N00014-91-J-1550

R&T Code: 413w003

Dr. John C. Pazik

Technical Report No. 20

Adsorption, desorption, and decomposition of HCl and HBr on Ge(100): Competitive pairing and near-first-order desorption kinetics

by

M. P. D'Evelyn, Y. L. Yang, and S. M. Cohen

Prepared for publication in the

Journal of Chemical Physics

Rensselaer Polytechnic Institute
Department of Chemistry
Troy, NY 12180

November 30, 1993

REPORT DOCUMENTATION PAGE

Form Approved
OMB No. 0704-0188

1. AGENCY USE ONLY (Leave blank)	2. REPORT DATE	3. REPORT TYPE AND DATES COVERED
	November 1993	Technical

4. TITLE AND SUBTITLE

Adsorption, desorption, and decomposition of HCl and HBr on Ge(100): Competitive pairing and near-first-order desorption kinetics

5. FUNDING NUMBERS

Grant #:
N00014-91-J-1550

6. AUTHOR(S)

M. P. D'Evelyn, Y. L. Yang, and S. M. Cohen

7. PERFORMING ORGANIZATION NAME(S) AND ADDRESS(ES)

Rensselaer Polytechnic Institute
Department of Chemistry
Troy, NY 12180

8. PERFORMING ORGANIZATION REPORT NUMBER

Technical Report
#20

9. SPONSORING/MONITORING AGENCY NAME(S) AND ADDRESS(ES)

Office of Naval Research
800 N. Quincy Street
Arlington, VA 22217-5000

10. SPONSORING/MONITORING AGENCY REPORT NUMBER

11. SUPPLEMENTARY NOTES

Prepared for publication in:
Journal of Chemical Physics

12a. DISTRIBUTION/AVAILABILITY STATEMENT

Approved for public release; distribution is unlimited.

12b. DISTRIBUTION CODE

13. ABSTRACT *(Maximum 200 words)*

We have investigated the surface chemistry of coadsorbed hydrogen and halogen atoms on Ge(100), produced by dissociative chemisorption of HCl and HBr, by temperature-programmed desorption. The initial sticking probability, S_0, for HCl decreases from 0.6 at a substrate temperature of 270 K to 0.05 at 400 K, indicative of a precursor state to adsorption. For HBr S_0 is constant at 0.7 over the same temperature range. A fraction f of adsorbed hydrogen atoms desorb associatively as H_2 near 570 K, while the remaining (1-f) H atoms recombine with adsorbed halogen atoms and desorb as the hydrogen halide (HX) near 580 - 590 K. The activation energies for desorption of H_2, HCl, and HBr are all approximately 40 kcal/mol. For both HCl and HBr f is 0.7 at low initial coverage and decreases slightly to 0.6 at saturation. The fraction f of adsorbed halogen atoms left on the surface following the competitive desorption of H_2 and HX desorb as the dihalides $GeCl_2$ and $GeBr_2$ near 675 K and 710 K, respectively. Desorption of H_2, HCl, and HBr occurs with near-first-order kinetics, similar to the behavior of hydrogen adsorbed alone, which we attribute to preferential pairing induced by the π bond on unoccupied Ge dimers. We introduce and solve a generalized doubly-occupied dimer model incorporating competitive pairing of H+H, H+X, and X+X on Ge dimers to explain the near-first order kinetics. The model quantitatively accounts for both the desorption kinetics and the relative yields of H_2 and HX with pairing energies of $\approx$ 3 kcal/mol. Implications of the present results for surface thermochemistry, chemical vapor deposition, and atomic layer epitaxy of Ge and Si (100)2×1 surfaces are discussed.

14. SUBJECT TERMS	15. NUMBER OF PAGES
Germanium, desorption kinetics, chemical vapor deposition, atomic layer epitaxy	16. PRICE CODE

17. SECURITY CLASSIFICATION OF REPORT	18. SECURITY CLASSIFICATION OF THIS PAGE	19. SECURITY CLASSIFICATION OF ABSTRACT	20. LIMITATION OF ABSTRACT

Adsorption, desorption, and decomposition of HCl and HBr on Ge(100): Competitive pairing and near-first-order desorption kinetics

Mark P. D'Evelyn,[a)]
Departments of Chemistry and Materials Engineering, Rensselaer Polytechnic Institute, Troy, NY 12180

Yuemei L. Yang, and
Department of Chemistry, University of Houston, Houston, TX 77004

Stephen M. Cohen
Zettlemoyer Center for Surface Studies, Lehigh University, Bethlehem, PA 18105

Abstract

We have investigated the surface chemistry of coadsorbed hydrogen and halogen atoms on Ge(100), produced by dissociative chemisorption of HCl and HBr, by temperature-programmed desorption. The initial sticking probability, S_0, for HCl decreases from 0.6 at a substrate temperature of 270 K to 0.05 at 400 K, indicative of a precursor state to adsorption. For HBr S_0 is constant at 0.7 over the same temperature range. A fraction f of adsorbed hydrogen atoms desorb associatively as H_2 near 570 K, while the remaining (1-f) H atoms recombine with adsorbed halogen atoms and desorb as the hydrogen halide (HX) near 580 - 590 K. The activation energies for desorption of H_2, HCl, and HBr are all approximately 40 kcal/mol. For both HCl and HBr f is 0.7 at low initial coverage and decreases slightly to 0.6 at saturation. The fraction f of adsorbed halogen atoms left on the surface following the competitive desorption of H_2 and HX desorb as the dihalides $GeCl_2$ and $GeBr_2$ near 675 K and 710 K, respectively. Desorption of H_2, HCl, and HBr occurs with near-first-order kinetics, similar to the behavior of hydrogen adsorbed alone, which we attribute to preferential pairing induced by the π bond on unoccupied Ge dimers. We introduce and solve a generalized doubly-occupied dimer model incorporating competitive pairing of H+H, H+X, and X+X on Ge dimers to explain the near-first order kinetics. The model quantitatively accounts for both the desorption kinetics and the relative yields of H_2 and HX with pairing energies of ≈ 3 kcal/mol. Implications of the present results for surface thermochemistry, chemical vapor deposition, and atomic layer epitaxy of Ge and Si (100)2×1 surfaces are discussed.

a) Author to whom correspondence should be addressed. Also affiliated with General Electric Corporate Research and Development, P. O. Box 8, Schenectady, NY 12301.

Submitted to *Journal of Chemical Physics*

I. INTRODUCTION

The surface chemistry of coadsorbed hydrogen and halogen atoms plays an important role in the growth of the group IV semiconductors silicon, Ge_xSi_{1-x} alloys, and diamond by chemical vapor deposition (CVD). Surface decomposition of chlorosilanes on silicon surfaces produces adsorbed H and Cl, and in fact chlorosilane CVD has historically been the dominant technology for epitaxial growth of silicon.[1] Similar techniques have recently been extended to growth of Ge_xSi_{1-x} alloys.[2] H/Cl surface chemistry has also been implicated in determining the distribution of crystallographic orientations that remain stable during silicon growth by CVD.[3] While diamond film growth by CVD typically involves hydrogen and hydrocarbons, several authors have reported improved results using alkyl halide precursors,[4,5] which may similarly involve coadsorbed hydrogen and halogen atoms. There is a great deal of current interest in the development of methods for atomic layer epitaxy (ALE) techniques[6] for group IV materials, and hydrogen-halogen chemistry offers a promising approach. Several techniques involving alternating cycles of a halogenated precursor and hydrogen have been proposed for ALE of silicon[7-12] and diamond.[5] Besides being important for growth, hydrogen-chlorine chemistry is also important in the etching of silicon.[13]

In addition to being technologically important, coadsorbed hydrogen and halogen atoms on semiconductor surfaces constitute an interesting model system from a fundamental point of view. Halogen atoms constitute perhaps the simplest adsorbates on semiconductor surfaces after hydrogen, and important phenomena such as ordering and intermixing of adsorbed species and the branching ratio between competing reaction channels can be investigated by coadsorption studies. To date, however, only a handful of researchers have investigated the interaction of hydrogen halides[14-20] or dichlorosilane (SiH_2Cl_2)[9,21] with silicon surfaces. On germanium, only very early hydrogen-halogen work[14,16,22] and our preliminary results[23,24] have been reported. Further interest in hydrogen-halogen surface chemistry stems from recent observations that atomic hydrogen can readily abstract halogen atoms from Si(100),[25-27] which is directly relevant to ALE.[5,9,11]

Much more attention has been devoted to the adsorption of hydrogen or halogen atoms individually. The structures of adsorbed hydrogen on Ge(100)[28-30] are directly analogous to those on Si(100),[30-33] the most stable species being the monohydride, with one hydrogen atom on each dimerized surface atom. Structures analogous to the monohydride were suggested by a photoelectron spectroscopic study of Cl and Br on Ge(100)2×1,[34] a picture which is supported by the corresponding structures of Cl[35,36] and Br[37] on Ge(111) and of Cl on Si(100)2×1.[35,38-40]

The mechanism, kinetics, and dynamics of hydrogen desorption from Si and Ge (100)2×1 surfaces have been the focus of a great deal of recent effort and also provided much of the

motivation for the present study. The desorption kinetics are nearly first order in the hydrogen coverage on both Si(100)[41-45] and Ge(100),[46] in contrast to the near-second-order behavior seen on the (111) faces[42,47,48] and on metals. The desorption kinetics of hydrogen from diamond (100) are also approximately first order.[49] Hydrogen molecules desorbing from Si(100) are vibrationally hot[50,51] but rotationally cold;[50,51] the angular distribution is peaked toward the surface normal[52] but the velocity distribution is approximately thermal.[53] The available experimental evidence seems to favor a sequential[32,51] desorption mechanism between H atoms paired on a single dimer.[42-46,49,51,54] The near-first-order kinetics can be explained by preferential pairing of adsorbed hydrogen,[43-46,54] which is driven by the π bond[55] on "unoccupied" surface dimers and has been observed directly by scanning tunneling microscopy (STM).[54] Fitting the deviation from first-order kinetics at low coverage to the predictions of our doubly-occupied dimer model[43] leads to estimates of 5-7 kcal/mol and $\approx$ 5 kcal/mol for the pairing energies of hydrogen on Si(100)[43-45] and Ge(100),[46] which is also a measure of the π bond strength on the clean surface.[43,46] These estimates of the pairing energy for hydrogen on Si(100) are also in reasonable agreement with values implied by recent Si-H bond strength calculations.[32,33] However, recent high-level quantum mechanical calculations of the desorption dynamics between paired hydrogen atoms[33,56,57] on Si(100)2×1 have arrived at activation energies much larger than the 57-58 kcal/mol observed experimentally.[42,44,45] The apparent discrepancy between theory and experiment remains to be resolved.

If preferential pairing of adsorbed species is indeed the explanation for the near-first-order desorption kinetics of hydrogen on diamond, Si, and Ge (100)2×1 surfaces, then virtually all recombinative desorption processes between mobile adsorbates on group IV (100)2×1 should be first order[43,54] since the driving force for pairing, the dimer π bond, is a property of the clean surface. The present study of the desorption kinetics of HCl and HBr from Ge(100), which occurs in competition with desorption of H_2, constitutes the first test of this prediction on an adsorbate other than hydrogen.

More limited information is available on the desorption kinetics of adsorbed halogens. Reactions of Cl_2[58] and Br_2[59] with Si(100) have been investigated by temperature-programmed desorption (TPD), and the corresponding reactions with Ge(100) have been investigated by reactive scattering.[60,61] At low initial halogen coverages or high reaction temperatures on Si or Ge (100) the dihalide is the dominant desorption (etch) product, while tetrahalide formation becomes important at higher initial coverage or lower reaction temperatures.

In this paper we report the adsorption kinetics of HCl and HBr on Ge(100) and the desorption kinetics and relative yields of H_2, HX, and GeX_2 (X=Cl or Br), as determined by temperature-programmed desorption (TPD). We introduce and solve a generalized doubly-occupied dimer

model that incorporates pairing between H, X, and H+X atoms on Ge-Ge surface dimers and competitive desorption of H_2 and HX, and show that the new model quantitively accounts for the data. However, the inferred pairing energies are smaller than that obtained for hydrogen adsorbed alone. The results are discussed within the context of estimates of the thermochemistry of adsorbed H, Cl, and Br on Ge and Si surfaces.

II. EXPERIMENTAL

Experiments were performed in an ultrahigh vacuum (UHV) chamber that is described in detail elsewhere.[62,63] Briefly, the chamber is pumped via a liquid-N_2-trapped diffusion pump and a titanium sublimation pump, and is equipped with LEED/ESDIAD optics, an Auger spectrometer (VSW hemispherical analyzer HA-100), a VG SXP-400 quadrupole mass spectrometer (QMS) with a water-cooled shroud mounted on a translation system, a calibrated gas doser,[64] and an ion gun. The base pressure of the apparatus was 1×10^{-10} Torr for the experiments reported here, but some of the experiments were performed at $\approx 7 \times 10^{-10}$ Torr with the titanium getter saturated. The sample holder was mounted on a rotatable *xyz* manipulator.

The Ge(100) sample was cleaved from a wafer (Si-Tech, Inc.) cut 4–6° off the (100) plane towards the [011] direction, 0.25–0.30 mm thick, n-type, ρ = 5–40 Ω cm, into a rectangle 13.4 mm × 13.8 mm. A chromel-alumel thermocouple was cemented into a small hole (~ 0.5 mm dia.) drilled near one edge of the sample using Aremco 516 high-temperature cement. The sample was mounted between Ta-foil clips attached to a Cu block and could be heated resistively to > 873 K and cooled with liquid nitrogen down to 153 K. The active area presented to the doser after mounting was 11.5 mm × 13.4 mm. After degreasing, the Ge sample was placed in the chamber and cleaned by several sputter-and-anneal cycles (i_{Ar^+} = 2–3 μA cm^{-2}, E_{Ar^+} = 500 V, T_{anneal} = 850 K).

Exposures to HCl or HBr were performed by rotating the sample to face the doser and admitting a known amount of gas to the chamber through a calibrated aperture. Computer calculations of the gas flux[65] show that, for this sample geometry, 17 % of the molecules leaving the doser strike the sample, yielding a flux of $(4.11 \pm 0.23) \times 10^{15}\ M^{-1/2}\ P\ s^{-1}$, where M is the molecular mass (g mol^{-1}), and P is the pressure (Torr) upstream of the conductance-limiting orifice[64] during a dose. For Ge(100), one monolayer (ML) = 6.23×10^{14} atoms cm^{-2}, and is used below to scale both doses and surface coverages. In control experiments, the sample was exposed to atomic hydrogen by backfilling the UHV chamber with H_2 to pressures of 2×10^{-8}–5×10^{-7} Torr and heating a coiled W filament located about 3 cm from the sample to 1700-1800 K.

All coverages were determined by TPD. A coverage calibration for surface hydrogen was obtained by TPD, detecting H_2 (m/e=2) following a saturation dose of H_2S. H_2S has been shown

to adsorb dissociatively on Ge(100) as H + SH[66] up to 0.5 ML coverage at saturation,[67] and yields exclusively H_2 and GeS as desorption products upon heating.[62] We used the same coverage calibration in a TPD study of the desorption of H_2 from Ge(100) following adsorption of atomic hydrogen,[23,46] and found that a shoulder at 525 K in the TPD peak appeared for coverages above 0.96 ML.[23] It is well established that an analogous lower-temperature TPD peak for H_2 desorbing from Si(100) appears for initial coverages greater than one monolayer,[41,45,51,68] corresponding to decomposition of dihydride (SiH_2) species, and that dihydride species on Ge(100) similarly decompose at a lower temperature than the GeH monohydride state.[29] The fact that the onset for the appearance of the shoulder occurs at one monolayer therefore supports the H_2S coverage calibration described above. HX (X = Cl or Br) coverages were determined by assuming that both molecules similarly reach a saturation coverage of 0.5 ML of H + X. This last assumption is examined critically in the discussion section below.

After dosing, when the background pressure returned to the background level, the sample was rotated to face the entrance slit of the water-cooled QMS shroud, at a distance of ≈ 0.5 cm. The temperature was ramped at a rate of 2 K s^{-1}, controlled by a Eurotherm temperature controller, and QMS signals, multiplexed for 1–3 masses, were recorded by an AT-compatible personal computer. We found that the most reproducible results, particularly with HCl, were obtained by letting the titanium sublimation pump become saturated and operating at a chamber pressure of 7-8 × 10^{-10} Torr. The reason for the improved reproducibility is presumably that the chamber pumping speed remained more nearly constant so that integrated TPD peaks were accurately proportional to the initial coverage regardless of the recent dosing history. Most of the H_2 and HX TPD results presented below were obtained with the Ti getter saturated. The sublimator was used when GeX_2 desorption data was collected separately, since the GeX_2 species are expected to condense on the chamber walls regardless of the presence or absence of a getter.

III. RESULTS

Three desorption products were observed following exposure to HX (X = Cl or Br): HX, H_2, and GeX_2, as shown in Figs. 1 and 2 for HCl and HBr, respectively. In both cases H_2 desorption occurs near 565 K after a saturation dose, as for desorption from hydrogen adsorbed alone[23,46] or following decomposition of H_2O or H_2S.[62] HCl or HBr desorption occurs concurrently with H_2 desorption, exhibiting peak temperatures near 575 and 585 K, respectively, at saturation initial coverage. Using the H_2S coverage calibration described above for the hydrogen coverage Θ_H, 0.30 ML and 0.31 ML of hydrogen atoms desorb as H_2 following saturation exposures to HCl and HBr, respectively. Assuming that the saturation coverage of both molecules is 0.5 ML, this implies that 0.20 and 0.19 ML of the hydrogen atoms desorb as HX for HCl and HBr, respectively. The

dihalide etch products $GeCl_2$ and $GeBr_2$ desorb at higher temperatures, 675 and 710 K, respectively, following saturation HX doses.

The magnitude of the peak desorption temperature for HCl and HBr provides a clear indication that the adsorption is dissociative, since molecular HCl and HBr could only physisorb to the surface and would be expected to desorb well below 300 K. However, to prove that the adsorption is dissociative we performed control experiments. Adsorbed Cl or Br were prepared on the surface by dosing with HCl or HBr, respectively, and flashing the sample to approximately 635 K. This procedure removes surface hydrogen as H_2 and HX (Figs. 1, 2), leaving adsorbed halogen atoms, and avoids the complexity of separate experiments with Cl_2 and Br_2. The sample was then rotated to face the W filament at 1700-1800 K and given a nominal dose of 10 L of molecular plus atomic hydrogen. The sample was then rotated to face the QMS and the temperature was ramped. In both cases an HX desorption peak was observed near 575 K. Since the latter experiment involved reaction between absorbed halogen and hydrogen atoms and yielded the same HX TPD peaks as shown in Fig. 1 and 2 following an exposure to HX, we conclude that adsorption of HX is indeed dissociative.

Initial sticking probabilities, S_0, for HCl and HBr were obtained from the slopes of coverage versus exposure data. For intermediate HX coverages, the coverage of hydrogen desorbing as H_2 was determined as the ratio of the integrated TPD peak intensity to that of H_2 following a saturation dose of H_2S, as described above. The coverage of hydrogen desorbing as HX was determined as the ratio of the integrated HX peak to that of HX following a saturation dose of HX multiplied by the inferred coverage of hydrogen desorbing as HX at saturation (0.20 or 0.19 ML for HCl or HBr, respectively). The sum of these two coverages is then the total amount of hydrogen initially chemisorbed and, by stoichiometry, the initial coverage of dissociated HX. We ran a number of spot checks to insure that the amount of desorbing H_2 and HX following a null dose was negligible. The initial sticking probability was then obtained as the initial slope of a plot of total HX coverage versus HX exposure, as determined using the calibrated doser described in the preceding section. The results for S_0 as a function of substrate temperature are summarized in Fig. 3. S_0 for HCl decreased from 0.6 at 270 K to 0.05 at 400 K, while that of HBr was constant at 0.7 over the same temperature range.

Stoichiometry implies that for every H_2 molecule that desorbs, the two X atoms remaining from dissociative adsorption of HX must desorb as GeX_2. The desorption peaks for H_2 and HX have a strong overlap while those of GeX_2 occur at higher temperature. Therefore, the branching ratio (H_2 + GeX_2 versus HX desorption) may be usefully described by the fraction f of adsorbed hydrogen atoms which desorb as H_2. The observed saturation coverages of hydrogen desorbing as H_2 of 0.30 and 0.31 ML for HCl and HBr, respectively, imply that f = 0.60 or 0.62 for HCl and

HBr from the assumed saturation HX coverage of 0.5 ML. At lower initial coverage of HCl or HBr f increases slightly to 0.66 and 0.68, respectively, in the low initial-coverage limit. However, we estimate the uncertainty in f as approximately 0.05, so the increase at low coverages may not be real.

TPD spectra for H_2 and HX as a function of the initial HX coverage are shown in Figs. 4 and 5 for HCl and HBr, respectively. In both cases H_2 desorption occurs near 562 K after a saturation dose, and the peak temperature T_p increases to about 580 K at initial coverages of 0.05 ML. For HCl and HBr desorption T_p increases from 578 and 583 K, respectively, at saturation initial coverage to 590 and 595 K at initial coverages of ≈0.05 ML. The weak dependence of T_p on initial coverage for both H_2 and HX desorption, together with the asymmetric peak shapes (Figs. 1,2,4, and 5), indicates near-first-order kinetics. The dependence of T_p for both H_2 and HX on the initial HX coverage is summarized in Figs. 6 and 7 for HCl and HBr, respectively, together with fits made using the model described in the next section.

We have not investigated the coverage dependence of the $GeCl_2$ and $GeBr_2$ desorption products in detail because the signal-to-noise ratio in the data was significantly worse than that for H_2 and HX and because the modification of the surface structure implied by the Ge atom removal associated with desorption complicates the interpretation of the results. We found that T_p for $GeCl_2$ was constant at 675 K to within 10 K for initial HCl coverages between 0.03 and 0.5 ML. For $GeBr_2$ T_p increased from 710 K at saturation coverage to 765 K at an initial HBr coverage of 0.05 ML. The desorption behavior of $GeCl_2$ is indicative of first-order kinetics while that of $GeBr_2$ suggests a kinetic order intermediate between 1 and 2.

IV. COMPETITIVE PAIRING MODEL

The near-first-order desorption kinetics of HX implied by the weak dependence of on initial coverage are qualitatively similar to the desorption behavior of hydrogen on Ge(100)2×1[46] and on Si(100)2×1.[41-45] As previously, for hydrogen adsorbed alone,[43,46] we attribute the near-first-order kinetics to preferential pairing of adsorbed atoms on surface dimers driven by the weak π bonds on clean surface dimers. The presence of two types of atoms (H, X), three types of pairing (H+H, H+X, X+X), and three desorption channels necessitates a generalization of the doubly-occupied dimer model that we developed to explain the desorption kinetics of hydrogen from Si(100)2×1[43] and is described below.

Consider a surface with M (2×1) dimer sites, each of which can be empty, or singly-occupied by H or X, or doubly-occupied by H+H, H+X, or X+X. Suppose that $2N_H$ hydrogen atoms and $2N_X$ halogen atoms are chemisorbed on the surface and that $N_H+N_X < M$, so that the (2×1)

reconstruction is undisturbed. For the present we assume that the dimers are non-interacting as in the original model.[43] We consider the effects of interactions between dimers for H on Si(100)2×1 elsewhere.[69,70] For simplicity let us assume that in the (degenerate) ground state of the system, all $2N_H$ hydrogen atoms are paired on N_H dimer sites and all $2N_X$ halogen atoms are paired on N_X dimer sites. Identical results are obtained if the ground state is instead assumed to consist of paired H+X atoms plus paired H or X atoms, whichever species is present in excess. Let ε_{HH} and ε_{XX} be the energies required to unpair the hydrogen or halogen atoms, respectively, that is, to move a H or X atom from a doubly-occupied to an empty dimer, creating two singly-occupied dimers, as indicated in Eqs. (1) and (2):

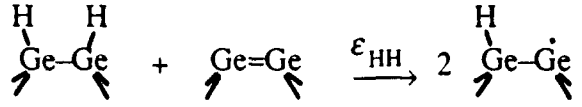

(1)

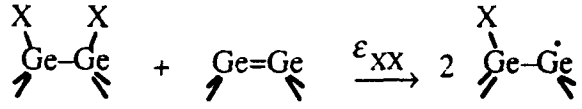

(2)

Suppose there are n_H and n_X such unpairings, respectively, in the system. The H and X atoms on singly-occupied dimers produced by unpairings of HH and XX dimers can pair up to form an HX doubly-occupied dimer; suppose there are n_{HX} such re-pairings. The energy gained by re-pairing of H+X is ε_{HX}, as indicated in Eq. (3):

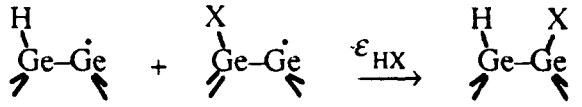

(3)

Define m_{HH}, m_{HX}, and m_{XX} to be the numbers of doubly-occupied dimers with paired H+H, H+X, or X+X atoms, respectively, m_{H*} and m_{X*} to be the numbers of singly-occupied dimers with H or X atoms, and m_{**} to be the number of unoccupied dimers. It is readily seen that

$$\begin{aligned} m_{HH} &= N_H - n_H \\ m_{XX} &= N_X - n_X \\ m_{HX} &= n_{HX} \\ m_{H*} &= 2n_H - n_{HX} \\ m_{X*} &= 2n_X - n_{HX} \\ m_{**} &= M - N_H - N_X - n_H - n_X + n_{HX} \end{aligned} \tag{4}$$

The partition function Z for this non-interacting lattice gas model is only marginally more complicated than that for a one-component system:[43]

$$Z = \sum_{n_H, n_X, n_{HX}} \frac{M!\ 2^{(m_{HX} + m_{H*} + m_{X*})}}{m_{HH}! m_{HX}! m_{XX}! m_{H*}! m_{X*}! m_{**}!} \exp\left[-\beta \left(n_H \varepsilon_{HH} + n_X \varepsilon_{XX} - n_{HX} \varepsilon_{HX} \right) \right] \tag{5}$$

where $\beta \equiv 1/k_B T$. The combinatorial factor arises from the number of ways of arranging the six type of dimers, and the $2^{(m_{HX} + m_{H*} + m_{X*})}$ factor takes account of the fact that H+X-occupied dimers and both H* and X* singly-occupied dimers can each be arranged in two different ways.

The equilibrium populations of the various dimer arrangements are obtained by maximizing the partition function. Approximating $\ln Z$ by the logarithm of the maximum summand, using Eqs. (4) to replace the numbers of dimers by the numbers of excitations n_H, n_X, and n_{HX}, and setting the partial derivatives of $\ln Z$ derivative with respect to n_H, n_X, and n_{HX} equal to zero, we obtain three equations in the three unknowns:

$$4 \exp(-\beta\varepsilon_{HH}) = \frac{(2n_H - n_{HX})^2}{(N_H - n_H)(M - N_H - N_X - n_H - n_X + n_{HX})} \tag{6a}$$

$$4 \exp(-\beta\varepsilon_{XX}) = \frac{(2n_X - n_{HX})^2}{(N_X - n_X)(M - N_H - N_X - n_H - n_X + n_{HX})} \tag{6b}$$

$$2 \exp(-\beta\varepsilon_{HX}) = \frac{(2n_H - n_{HX})(2n_X - n_{HX})}{n_{HX}(M - N_H - N_X - n_H - n_X + n_{HX})} \tag{6c}$$

We now introduce the coverages of hydrogen and halogen atoms, expressed with respect to the number of dangling-bond sites and coverages of the various types of doubly-occupied and singly-occupied dimers:

$$\begin{aligned}
\Theta_H &= N_H/M \\
\Theta_X &= N_X/M \\
\Theta_{HH} &= m_{HH}/M \\
\Theta_{XX} &= m_{XX}/M \\
\Theta_{HX} &= m_{HX}/M \\
\Theta_{H*} &= m_{H*}/M \\
\Theta_{X*} &= m_{X*}/M \\
\Theta_{**} &= m_{**}/M
\end{aligned} \tag{7}$$

Re-introducing the dimer numbers defined in Eq. (4) into Eqs. (6) and introducing the coverages defined in Eq. (7), we obtain three rather simple equations:

$$4 \exp(-\beta\varepsilon_{HH}) = \frac{\Theta_{H*}^2}{\Theta_{HH}\Theta_{**}} \tag{8a}$$

$$4 \exp(-\beta\varepsilon_{XX}) = \frac{\Theta_{X*}^2}{\Theta_{XX}\Theta_{**}} \tag{8b}$$

$$2 \exp(-\beta\varepsilon_{HX}) = \frac{\Theta_{H*}\Theta_{X*}}{\Theta_{HX}\Theta_{**}} \tag{8c}$$

Eqs. (8) may be solved most conveniently by choosing as the three independent variables Θ_{HX}, Θ_{H*}, and Θ_{X*}. It is easily seen that the remaining dimer coverages can be expressed in terms of these three together with the total hydrogen and halogen coverages, Θ_H and Θ_X, respectively, by

$$\Theta_{HH} = \Theta_H - \frac{1}{2}(\Theta_{H*} + \Theta_{HX}) \tag{9a}$$

$$\Theta_{XX} = \Theta_X - \frac{1}{2}(\Theta_{X*} + \Theta_{HX}) \tag{9b}$$

$$\Theta_{**} = 1 - \Theta_H - \Theta_X - \frac{1}{2}(\Theta_{H*} + \Theta_{X*}) \tag{9c}$$

Eq. (8c) may then be trivially solved to obtain Θ_{HX} in terms of Θ_{H*} and Θ_{X*}:

$$\Theta_{HX} = \frac{1}{2}\exp(\beta\varepsilon_{HX})\frac{\Theta_{H*}\Theta_{X*}}{\Theta_{**}} \tag{10}$$

where Θ_{**} is given by Eq. (9c). Unfortunately, Eqs. (8a) and (8b) do not simplify further, leaving two coupled equations in the unknowns Θ_{H*} and Θ_{X*} which must be solved numerically.

Solution of Eqs. (8-10) yields the coverages of each possible combination of species adsorbed on dimers for a specified total hydrogen and halogen coverage at a given temperature. All that remains to be able to simulate the TPD data is to postulate a relationship between the dimer coverages and the desorption rates.

We postulate, as before,[43,46] that desorption occurs between atoms paired on a single dimer, which in this case includes H+X as well as H+H. The desorption rates of H_2 and HX are then given by $k_{HH}\Theta_{HH}$ and $k_{HX}\Theta_{HX}$, respectively, where k_{HH} and k_{HX} are the rate constants for desorption of H_2 and HX, respectively. We neglect desorption of GeX_2 since it occurs at higher temperature and we seek to model only the competitive desorption of H_2 and HX. The kinetic equations for the surface coverage during a TPD experiment are then

$$\frac{d\Theta_H}{dt} = -k_{HH}\Theta_{HH} - k_{HX}\Theta_{HX} \tag{11a}$$

$$\frac{d\Theta_X}{dt} = -k_{HX}\Theta_{HX} \tag{11b}$$

We assume that the preexponential factor for k_{HH} is 2×10^{15} sec^{-1}, as was found for H_2 desorption from Si(100) by Höfer *et al.*,[44] who took H-atom pairing into account in the analysis, and a value of 10^{13} sec^{-1} for the preexponential factor for k_{HX}. As discussed elsewhere,[46] the dependence of TPD peak temperature on coverage is quite insensitive to the value of the preexponential factor. The TPD peak temperatures for H_2 and HX at high initial coverage then imply activation energies of approximately 42 and 38 kcal/mol for k_{HH} and k_{HX}, respectively.

Simulated TPD experiments at initial coverages of $\Theta_H = \Theta_X$ between 0 and 0.5 ML began at a surface temperature of 450 K, which was then ramped linearly at 2 K s^{-1} as in the experiments. At each temperature, the equilibrium surface dimer coverages (Eqs. 7) were calculated by solving Eqs. (8-10) numerically, evaluating the rate constants k_{HH} and k_{HX}, and calculating the time derivatives of Θ_H and Θ_X (Eqs. 11). The use of equilibrium dimer coverages assumes, of course, that surface diffusion is sufficiently fast relative to desorption for quasiequilibrium to be maintained even as paired hydrogen and H+X are removed by desorption (Eq. 11). The dynamic surface coverages $\Theta_H(t)$ and $\Theta_X(t)$ were generated in tandem using a 4th order Runge-Kutta integration scheme. The desorption rates for H_2 and HX were stored at each time step. The time increment was chosen so that the surface temperature increases by 1 K at each step, which we found to yield converged results. As H_2 desorbs the surface becomes increasingly enriched in X relative to H ($\Theta_H < \Theta_X$). After each run, the peak temperatures T_p for H_2 and HX and the fraction f of hydrogen desorbing as H_2 were evaluated. The pairing energies were then determined by performing a least-squares fit between measured and predicted values of the peak temperature and H_2 yields. The activation energies for k_{HH} and k_{HX}, $E_{a,HH}$ and $E_{a,HX}$, respectively, were also allowed to vary so as to allow for small shifts in T_p, with the rationale that coadsorbed halogen atoms may slightly perturb the desorption kinetics.

Excellent agreement between experiment and model predictions for both HCl and HBr was obtained by assuming equal values for ε_{HH}, ε_{HX}, and ε_{XX}. For HCl best agreement was obtained from $\varepsilon_{HH} = \varepsilon_{HX} = \varepsilon_{XX} = 2.7$ kcal/mol, $E_{a,HH} = 41.4$ kcal/mol, and $E_{a,HX} = 38.1$ kcal/mol. With these parameters the fraction f of surface hydrogen desorbing as H_2 is 68% at 0.5 ML initial coverage and increases very slightly at lower coverage (69% at 0.05 ML). The model predictions for T_p are plotted together with the experimental results in Fig. 6. The corresponding best parameter values for HBr are $\varepsilon_{HH} = \varepsilon_{HX} = \varepsilon_{XX} = 2.8$ kcal/mol, $E_{a,HH} = 41.7$ kcal/mol, and $E_{a,HX} = 38.5$ kcal/mol. The predicted values of T_p for H_2 and HBr are shown in Fig. 7 with the data. For HBr f is calculated as 69% at 0.5 ML initial coverage and again increases very slightly at lower coverage (70% at 0.05 ML). Agreement between experimental and model results, for T_p, f, and their coverage dependences, is quite good for both HCl and HBr. The results of fits obtained using different choices of parameters are discussed below.

V. DISCUSSION

A. Adsorption

The adsorption kinetics for HCl and HBr on Ge(100) are consistent with the paradigm we have proposed[43,62,71] for surface chemistry on group IV (100)2×1 surfaces: the dimerized surface

atoms are analogous to highly strained digermenes (compounds containing Ge-Ge double bonds), disilenes (Si=Si compounds), or olefins on Ge(100), Si(100) or diamond (100), respectively. If reaction occurs on a single surface dimer, adsorption and desorption are analogous to molecular addition and elimination reactions, respectively. Disilene and digermene compounds have been known for more than a decade, being synthesized for the first time in 1981[72] and 1982,[73] respectively. The π bonds in these molecules are considerably weaker than in olefins and readily undergo addition reactions with HCl, halogens, water, and alcohols. Several excellent reviews of disilene and digermene chemistry are available.[74]

The high sticking probabilities for HCl and HBr on Ge(100) (Fig. 3) imply negligible activation energies for adsorption of both molecules. The absence of an activation barrier suggests that adsorption occurs through four-center transition states on a single surface dimer,[62] so that Ge-H and Ge-X bonds can begin to form before the H-X bond is broken:

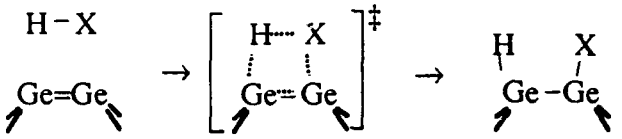

(12)

Simple geometric considerations suggest that dissociation of HX across a single dimer occurs more readily than between dangling bonds on adjacent dimers. The Ge=Ge dimer bond length on the clean surface may be estimated as 2.41 Å from the measured value of its parallel component (2.34 Å)[75] and the buckling angle (14°) calculated by high-level density functional theory.[76] The bond lengths in HCl (1.27 Å) and HBr (1.41 Å) are shorter than the Ge=Ge dimer bond, and therefore bond strain will be present in the transition state (Eq. 12). Ge atoms in adjacent dimers in the same row are separated by a considerably larger distance (3.99 Å). The HX bond would need to be nearly broken before Ge-H and Ge-X bonds on adjacent dimers could be formed, which should be accompanied by a substantial activation energy. Dissociative adsorption on a single dimer therefore seems more likely. The Ge-Ge dimer bond length is intermediate between the bond length in molecular digermenes, 2.21–2.35 Å,[73,77] and the single bond length of 2.44 Å in bulk germanium, as would be expected for a highly strained double bond. Ge surface dimers should therefore be even more reactive than molecular digermenes. Silicon and diamond surface dimers likewise should be substantially more reactive than the analogous disilene and olefin compounds. Four-center transition states for molecular addition reactions with π-bonded silicon and germanium compounds have been proposed since the early 1960's,[78,79] and therefore it is reasonable to suppose that similar transition state configurations occur during dissociative adsorption on π-bonded surface dimers. Although we have represented the transition state as being nearly symmetric for ease of visualization, the HX moiety is likely to be tilted and shifted toward one end

of the dimer, with the Ge-X distance being longer than Ge-H distance, based on the analogous transition state calculated for addition of HCl to $H_2Si{=}SiH_2$.[79]

The decrease of S_0 for HCl with surface temperature is analogous to the behavior seen for H_2O on Ge(100)[62,80] and suggests the existence of a mobile physisorbed precursor state.[81] The classical precursor model of Kisliuk,[81] which assumes thermalization of physisorbed molecules in a "precursor" state, predicts a temperature-dependent initial sticking probability given by

$$S_0(T) = \frac{\alpha}{1 + \nu_d/\nu_c \exp[-(E_d - E_c)/RT]} \qquad (13)$$

In Eq. (13), the trapping probability α is the probability that the incident molecule becomes "trapped" into the physisorbed precursor state, ν_d and ν_c are the preexponential factors for desorption and chemisorption, respectively, from the precursor state, and E_d and E_c are the corresponding activation energies. In the absence of a direct measurement of α for HCl on Ge(100), we simply assume $\alpha = 1$. The best fit to the data is then obtained with values of 7×10^4 for ν_d/ν_c and 6.3 kcal/mol for E_d-E_c. The fit is shown together with the data in Fig. 3. The modest value of E_d-E_c is typical for precursor adsorption systems. Only a limited significance should be ascribed to these precursor model parameters due to the uncertainty in the data and the oversimplification of the adsorption dynamics by the model.

While the temperature independence of S_0 for HBr could be explained by a precursor model with E_d fortuitously equal to E_c, we suggest that a more likely explanation is that E_c, the activation energy for dissociative chemisorption for physisorbed HBr, is approximately equal to zero. In this case incoming molecules would never thermalize into a physisorbed state but would simply dissociate at an adsorption site once enough translational energy had been dissipated to the lattice for the molecules to become localized. S_0 would simply equal α, where now α is interpreted as the fraction of incoming molecules that lose enough translational energy to the surface during the initial collision to undergo subsequent "bounces."

Why is S_0 for HBr on Ge(100) larger and E_c apparently smaller than the corresponding quantities for HCl? The simplest explanation would be a larger heat of adsorption for HBr, since the more exothermic of a pair of similar chemical reactions typically has the smaller activation energy.[82] However, estimates based either on bond strengths in analogous molecules or on the activation energies for desorption of HCl and HBr lead to the conclusion that the heats of adsorption of HCl and HBr on Ge(100) are very nearly equal, as discussed below. In addition, a direct calorimetric measurement of the heat of adsorption on polycrystalline Ge powder yielded nearly identical values for HCl and HBr.[16] We suggest an alternate simple explanation for the difference in S_0, motivated by the hypothetical transition state (Eq. 12). Because the H-Br bond is longer than

the H-Cl bond, less distortion is necessary to achieve the significant orbital overlap with the orbitals on the Ge dimer atoms necessary for a low-energy transition state. In addition, the force constant for the H-Br bond is 20% smaller than that for HCl,[83] so that the necessary distortion costs less energy. Further experiments on the reactivity of homologous molecules with Ge(100) and Si(100) are needed to determine whether this line of reasoning is capable of predicting trends in sticking probabilities correctly.

Independent evidence for dissociative adsorption across single dimers on Si(100)2×1, consistent with the adsorption model depicted in Eq. (12), comes from recent investigations of water adsorption by scanning tunneling microscopy (STM).[84,85] Two recent studies have provided clear evidence that many or most of the defects previously observed on Si(100)[86] and presumed to be intrinsic are in fact products of water adsorption.[84,85] The most prevalent of these "dark" sites are dimers, suggesting that dissociative adsorption as H+OH on a single dimer is the most common adsorption mechanism. The STM images also provide evidence for adsorption on adjacent dimers,[84,85] including isolated dangling bonds of low reactivity that were left over when most pairs of adjacent dangling bonds became saturated.[84] We note that dissociation fragments produced on a single dimer could become localized on adjacent dimers even at low temperature if exothermic bond formation during the chemisorption process causes a transient local heating, enabling one species to hop to an adjacent dimer.

We believe that the applicability of the molecular paradigm (Eq. 12) for the surface reactivity of Ge(100) and Si(100) should be examined in further detail to determine whether it can consistently rationalize reactivity trends. If it can, predictive capability should be possible, which could be useful to a wide variety of semiconductor growth and processing applications.

B. Desorption of H_2, HCl, and HBr and thermochemical estimates

By detailed balance, if adsorption of HCl and HBr occurs on a single Ge-Ge surface dimer (Eq. 12) then the reverse process, desorption, will occur between paired H+Cl or H+Br on a single dimer, as was explicitly assumed in the competitive pairing model described in section IV. A local picture for the desorption process is strongly supported by the insensitivity of the kinetics of H_2 desorption from Ge(100) to coverages of Cl, Br, O, or S as high as 0.5 ML (produced by dissociative adsorption of HCl, HBr, H_2O, or H_2S)[46,62] This insensitivity to coadsorbed species contrasts strongly with desorption kinetics on metal surfaces, where bonding is much more delocalized, which are often strongly perturbed by even a few percent of a monolayer of coadsorbed species.

The central conclusion of this paper is that preferential pairing of adsorbed H and X must be postulated in order to account for the near-first-order desorption kinetics. We have shown that the competitive pairing model accurately accounts for both the coverage dependence of T_p and the relative yields of H_2 and HX with pairing energies of H+H, H+X, and X+X of about 3 kcal/mol. To assess the robustness of the overall conclusion and the pairing energies we have performed a number of additional calculations. The sensitivity of the fits of the HCl data to the assumed pairing energies is illustrated in Fig. 8. Here the common pairing energies were fixed at 1, 2.7, and 5 kcal/mol and the activation energies for desorption, $E_{a,HH}$ and $E_{a,HX}$, were adjusted slightly for the best fit to the data. It is clear that significantly larger or smaller pairing energies yield a much poorer fit to the data. We estimate an uncertainty of ±1 kcal/mol in the common effective pairing energy.

Although our data are insufficient to establish how nearly equal the pairing energies ε_{HH}, ε_{HX}, and ε_{XX} are to one another, we can say that ε_{HX} must be comparable in magnitude to ε_{HH}. In other words, the data cannot be fit by assuming preferential pairing of hydrogen only. Shown in Fig. 9 are the results of fits to the HCl data made assuming that one or both of ε_{HX} and ε_{XX} are zero. If both ε_{HX} and ε_{XX} are set equal to zero, a noticeably worse fit to the dependence of T_p on Θ_0 is obtained (dashed curves). However, the most serious deficiency of a fit omitting preferential pairing of HX (i.e., $\varepsilon_{HX} = 0$) is that the coverage independence of T_p for HX can only be reproduced if nearly all the hydrogen desorbs as H_2 (i.e., $f \approx 1$) so that HX desorption becomes pseudo first order. An improved fit to the T_p data incorporating preferential pairing only of hydrogen can only be obtained with even worse agreement with the H_2 yields. We thus conclude that ε_{HX} is comparable in magnitude to ε_{HH}. A less definitive statement is possible whether ε_{XX} is comparable in magnitude to ε_{HH} and ε_{HX}. The fit to the T_p data assuming $\varepsilon_{XX} = 0$ and equal values of ε_{HH} and ε_{HX} (solid curves) is better but still inferior to the case where all the pairing energies are equal (Fig. 6). The predicted yields in this case are good, as is the dependence of T_p on Θ_0 for HCl. However, the predicted values of $T_p(\Theta_0)$ for H_2 exhibit a much stronger curvature than that seen experimentally or that predicted by the competitive pairing model with $\varepsilon_{HH} = \varepsilon_{HX} = \varepsilon_{XX}$. We thus conclude that ε_{XX} is also nonzero, but cannot make a definitive statement as to how close in magnitude it is to the other pairing energies.

It is not clear whether any inference about the value of ε_{XX} can be made from the desorption kinetics of GeX_2. Each desorption event removes one Ge atom from the surface, presumably disrupting the dimer structure. This will affect the driving force for pairing and also the surface mobilities, as diffusion along the dimer rows is likely to be more facile that diffusion perpendicular to them. Annealing of the Ge surface will also occur at these temperatures, but in the absence of evidence that annealing of the etch damage is fast in comparison to desorption we believe that an analysis of the desorption kinetics of GeX_2 based on an ideal-dimer model is not justified.

Finally, we have also fit the data using a phenomenological desorption model wherein pairing is not treated explicitly, as described in more detail elsewhere.[24] Rather then assuming that the desorption rates of H_2 and HX are $k_{HH}\Theta_{HH}$ and $k_{HX}\Theta_{HX}$, respectively, we set these quantities equal to $k_{HH}\Theta_H^n$ and $k_{HX}\Theta_H^m\Theta_X$. The rate constants k_{HH} and k_{HX} have the same meaning as in the competitive pairing model, but pairing is treated indirectly via the phenomenological reaction orders n and m. With these substitutions, the kinetic equations for the surface coverage during a TPD experiment become

$$\frac{d\Theta_H}{dt} = -k_{HH}\Theta_H^n - k_{HX}\Theta_H^m\Theta_X \quad (14a)$$

$$\frac{d\Theta_X}{dt} = -k_{HX}\Theta_H^m\Theta_X \quad (14b)$$

The simulation of TPD experiments was otherwise carried as for the competitive pairing model. The preexponential factor for HX, A_{HX}, was allowed to vary along with n and m, while the prexponential factor for H_2 was fixed as 2×10^{15} s^{-1} and both $E_{a,HH}$ and $E_{a,HX}$ were set equal to 42 kcal/mol. Fits roughly comparable in quality to those of the competitive pairing model were obtained for the coverage dependence of T_p for both H_2 and HX and the relative desorption yields. For HCl the best-fit parameters were $n = 1.2$, $m = 0.4$, and $A_{HX} = 5 \times 10^{14}$ s^{-1}. For HBr the corresponding values were $n = 1.35$, $m = 0.5$, and $A_{HX} = 4 \times 10^{14}$ s^{-1}.

Although the underlying physics of the phenomenological model are not explicit, the conclusion from the fitting is the same as with the competitive pairing model: correlation of both H+H and H+X is necessary to fit the data. The parameter n is the kinetic order for H_2 desorption. The vales of n close to 1 reflect the nonrandom distribution of H atoms and concomitant near-first-order desorption kinetics. A good fit could not be achieved with $m = 1$, which would imply random distributions of H and X: $\Theta_{HX} = \Theta_H\Theta_X$. Values of m less than one correspond to correlation of adsorbed H and X atoms ($m = 0$ would imply perfect correlation--$\Theta_{HX} = \Theta_H$--neglecting the fact that $\Theta_X > \Theta_H$ once H_2 desorption begins).

The relative yields of H_2 and HX constitute an important input to the competitive pairing model, and it is important to critically examine our assumption of a 0.5 ML saturation coverage for HX and to assess the sensitivity of the inferred preferential pairing energies to this assumption. Saturation coverages have been reported for a number of hydrides on Ge(100) and Si(100), and nearly all of them are approximately equal to 0.5 ML. Examples include H_2O[87] and H_2S[67] on Ge(100) and H_2O,[88] H_2S,[89] NH_3,[90] C_2H_2,[91] and C_2H_4[91] on Si(100). The only exception to the pattern of 0.5 ML saturation coverages of small hydrides on Si(100) or Ge(100) of which we are aware of is HCl on Si(100), whose adsorption has been reported to saturate at 0.25 ML.[20] A saturation coverage of 0.5 ML would be expected from dissociative adsorption of hydrides AH_x as

H and AH_{x-1} on surface dimers (Eq. 12), or from di-σ bond formation in the case of C_2H_2 and C_2H_4. Recent careful kinetic uptake measurements on some of these systems indicate saturation coverages of slightly less than 0.5 ML, viz., 0.37 ML for C_2H_2 and C_2H_4 on Si(100).[91] Saturation coverages slightly less than one molecule per surface dimer could result from steric repulsion, from surface defects, or from occasional dissociative adsorption events across dangling bonds on adjacent dimers rather than on a single dimer. The latter would result in isolated dangling bonds that may be relatively inert against adsorption.[84] On Ge(100), saturation coverages of both Cl and Br have been reported as 1 ML,[34] so steric repulsion as a limiting factor in HX adsorption seems unlikely. The use of relative TPD yields to determine coverages, as in this study, should reduce or eliminate the effect of non-adsorbing defect sites, since they should adsorb neither the calibration molecule (H_2S in the present case) nor the molecule under study (HX). Our measured yields of 0.30 and 0.31 ML of H_2 desorbing following saturation exposures to HCl and HBr, respectively, excludes a saturation coverage of 0.25 ML. Based on the evidence just summarized, it appears most likely that the saturation coverages of HCl and HBr on Ge(100) are slightly less than 0.5 ML.

While determination of the precise saturation coverages of HCl and HBr on Ge(100) will require further study, we find that our conclusions of preferential pairing of H+X as well as of H+H are not sensitive to the precise saturation coverage. If the saturation coverage of HCl were only 0.4 ML, the observed yield of 0.30 ML of surface hydrogen desorbing as H_2 would imply that 0.10 ML of hydrogen desorbs as HCl. The fraction f of surface hydrogen desorbing as H_2 would increase slightly from 0.75 at saturation coverage to 0.79 at an initial coverage of 0.05 ML. A least-squares fit to the T_p data for H_2 and HCl (with the initial coverages scaled downward as appropriate) using the modified yields produced agreement with the data nearly as good as that in Fig. 6, with f in the range of 0.75-0.74 for coverages between 0.04 and 0.4 ML. The parameters obtained in the modified fit were $\varepsilon_{HH} = \varepsilon_{HX} = \varepsilon_{XX} = 2.85$ kcal/mol, $E_{a,HH} = 41.2$ kcal/mol, and $E_{a,HX} = 38.4$ kcal/mol. The inferred pairing energy is nearly identical to that obtained assuming 0.5 ML saturation coverage (2.7 kcal/mol) and well within the ± 1 kcal/mol uncertainty. We thus conclude that the uncertainty in the actual saturation coverage of HX contributes only a slight uncertainty to the inferred pairing energies.

Our analysis of the TPD results idealizes the surface as being perfectly flat. However, the sample is tilted 4-6° from (100) and consequently 7-10% of the surface atoms are at step edges. While it would be worthwhile to quantify the effects of steps on desorption kinetics from (100)2×1 semiconductor surfaces, we argue that these effects are minor and do not substantially affect our conclusions. First, in the only directly analogous system for which data is available, Boland found that the spatial distribution of (paired) hydrogen atoms desorbing from Si(100)2×1 is *uncorrelated* with steps or defects.[54,92] Sites vacated by desorbing H_2 following brief annealing cycles of

Si(100)2×1:H were imaged by STM. At high hydrogen coverages desorption events occurred at random surface positions, while at lower coverages the remaining hydrogen tended to form one-dimensional chains due to effective interactions between doubly-occupied dimers.[54,69,70,92] At all coverages examined, however, there was no significant correlation between desorption sites and step edges.[54,92] Second, comparative studies of adsorption of several molecules, including H_2O,[84,89,93] H_2S,[89] Cl_2,[40] C_2H_4,[94] C_2H_2,[95] and HCOOH,[96] on flat and stepped Si(100)2×1 found no significant effect of the steps upon adsorption. By detailed balance, desorption cannot take place preferentially at steps unless adsorption leads to preferential population of step sites. Finally, if H and/or X adsorbed preferentially at steps these sites would remain saturated at coverages above 7-10% (the step density) and could not affect either the TPD peak temperature nor the H_2 versus HX yield at higher initial coverages. Since the data used to infer the effective pairing energies in the model were for coverages above 0.1 monolayer (cf. Figs. 6, 7), we conclude that steps make at most a minor contribution to the observed behavior.

Having concluded that preferential pairing of H+X occurs just as for H+H on Ge(100), that is, that ε_{HH} and ε_{HX} (and, probably, ε_{XX}) are greater than 0, we now turn to the implications of the fitted values of ε. If the π bond on surface Ge-Ge dimers provides the driving force for preferential pairing, then one might expect that ε_{HH}, ε_{HX}, and ε_{XX} would be very nearly equal to ε_{HH} for hydrogen adsorbed alone, or approximately 5 kcal/mol.[46] ε_{HX} and ε_{XX} might be reduced somewhat because of steric and/or electrostatic repulsion between the paired adsorbate atoms, particularly ε_{XX}, but ε_{HH} would be expected to be the same as when no halogen atoms were present. Just as we are able to conclude that the pairing energies (2.75 ± 1 kcal/mol) are greater than zero (Figs. 8, 9), it is also clear that they are less than 5 kcal/mol (Fig. 8). Several explanations are possible why the effective pairing energies are less than 5 kcal/mol, which cannot be resolved at present. One possibility is that ε_{HH} is close to 5 kcal/mol and ε_{HX} and ε_{XX} are less due to steric and electrostatic effects and that the fits are not able to distinguish this case from the equal-ε one. Experimentation with fits with various pairing energies suggests this is not the case, however: inferior fits are obtained with ε_{HH} = 5 kcal/mol. A second possibility is that the presence of coadsorbed halogen atoms does in fact reduce the driving force for pairing (recall that excess halogen atoms remain on the surface during a TPD ramp while H_2 and HX desorb). Such a reduction might occur because the more electronegative halogen atoms withdraw electron density from the surface, which decreases the population of the π band state. Another possibility is that the adsorbed halogen atoms cause a breakdown of quasiequilibium. If the halogen atoms are less mobile than adsorbed H atoms, they may not be able to reach the equilibrium extent of pairing during a TPD ramp. In addition, since diffusion along the dimer rows constitutes a quasi-one-dimensional system, they may also block diffusion H atoms and impede pairing of H+H and H+X.

Further study will be necessary to determine the origin of the quantitative differences between pairing of H+H adsorbed alone and in the HX system.

Estimates of the heats of adsorption of HCl and HBr can be obtained from both the desorption kinetics and from molecular bond energies. By detailed balance, the activation energy for desorption of HCl or HBr should be equal to the heat of adsorption plus the activation energy for adsorption. The near-unit values of S_0 imply that the latter is very small, as discussed above, so the heat of adsorption is approximately 40 kcal/mol for both HCl and HBr on Ge(100).

Independendent estimates of the heats of adsorption based on molecular bond energies are instructive but are limited by the paucity of accurate thermochemical data for germanium compounds. Dissociative adsorption of HX yields new Ge-H and Ge-X bonds and breaks the H-X bond and the Ge-Ge π bond on the dimer. The Ge-H bond energy in GeH_4 has been measured as 82 kcal/mol.[97] However, by analogy to silicon, replacement of the other Ge-H bonds in GeH_4 by bonds to other germanium atoms on Ge(100) is likely to reduce the Ge-H bond strength on the surface. The Si-H bond energy in $((CH_3)_3Si)_3Si$-H (79 kcal/mol[98]) is 12% weaker than that in SiH_4 (90 kcal/mol[99]). Assuming that a similar reduction occurs for germanium, we arrive at an estimate of 72 kcal/mol for the Ge-H bond energy on a (doubly-occupied) Ge(100) dimer. Reliable germanium-halogen bond strengths are not available, and for the surface Ge-Cl and Ge-Br bonds we use tabulated average bond energies of 81 and 66 kcal/mol, respectively.[100] For the π bond strength in Ge-Ge surface dimers we use 5 kcal/mol, as inferred from the departure of the desorption kinetics from first order at low coverage for hydrogen adsorbed alone.[46] The bond energies of H-Cl and H-Br are 103 and 88 kcal/mol, respectively.[101] We thus arrive at 72 + 81 - 103 - 5 = 45 kcal/mol for the heat of adsorption of HCl on Ge(100), and 72 + 66 - 88 - 5 = 45 kcal/mol for the heat of adsorption of HBr.

The similarity in the heat of adsorption and activation energies for desorption of HCl and HBr on/from Ge(100) are in agreement with an early calorimetric measurement on polycrystalline Ge powder. The bond strength calculation also makes clear that this similarity results from the weakening of the surface Ge-Br bond relative to that of Ge-Cl being very nearly equal to the difference in bond energies between H-Cl and H-Br. The near agreement of the bond strength estimates with the activation energies for desorption suggests that the bond strength estimates are individually reasonably accurate. More accurate determinations will be necessary, however, for specific inferences to be made about individual surface bond strengths.

Preferential pairing, which the available evidence suggests is a general phenomenon in adsorption on Si(100) and Ge(100), will affect the spatial distribution of adsorbed species during film growth by chemical vapor deposition or atomic layer epitaxy. If the gas phase growth species

is a stable molecule, two adjacent sites on a surface dimer will be necessary for dissociative chemisorption to occur. If most of the dangling bonds (and adsorbed species) are paired, larger saturation coverages will be possible with shorter exposures than would be the case is the distribution of dangling bonds on the surface were random. Near-unit saturation coverages would be particularly helpful for atomic layer epitaxy processes. However, the 3-5 kcal/mol pairing energies inferred from the desorption kinetics are small enough so that at typical growth temperatures pairing occurs to a substantial but incomplete extent. Independent measures of preferential pairing could provide further insight into this phenomenon and its usefulness for self-limiting processing chemistry for semiconductor surfaces.

ACKNOWLEDGMENTS

The authors acknowledge the Office of Naval Research for financial support of this work and the National Science Foundation (Grant CHE-8715812; the computational facilities were procured with funds from grant CHE-8909777) for additional support. We also thank Ms. Terttu Hukka for contributions to the initial phase of this project.

REFERENCES

1. For example, A. Sherman, *Chemical Vapor Deposition for Microelectronics* (Noyes Press, Park Ridge, New Jersey, USA, 1987).

2. (a) J. L. Hoyt, C. A. King, D. B. Noble, C. M. Gronet, J. F. Gibbons, M. P. Scott, S. S. Laderman, S. J. Rosner, K. Nauka, J. Turner, and T. I. Kamins, Thin Solid Films **184**, 93 (1990); (b) P. M. Garone, J. C. Sturm, P. V. Schwartz, S. A. Schwartz, and B. J. Wilkins, Appl. Phys. Lett. **56**, 1275 (1990); (c) T. O. Sedgwick and P. D. Agnello, J. Vac. Sci. Technol. A **10**, 1913 (1992).

3. J. G. E. Gardeniers and L. J. Giling, J. Cryst. Growth **115**, 542 (1991), and references therein.

4. (a) D. E. Patterson, B. J. Bai, C. J. Chu, R. H. Hauge, and J. L. Margrave, in *New Diamond Science and Technology*, edited by R. Messier, J. T. Glass, J. E. Butler, and R. Roy (Materials Research Society, Pittsburgh, PA, USA, 1991), p. 433; (b) R. A. Rudder, G. C. Hudson, J. B. Posthill, R. E. Thomas, and R. J. Markunas, Appl. Phys. Lett. **59**, 791 (1991); (c) M. Kadano, T. Inoue, A. Miyanaga, and S. Yamazaki, Appl. Phys. Lett. **61**, 772 (1992); (d) B. J. Bai, C. J. Chu, D. E. Patterson, R. H. Hauge, and J. L. Margrave, J. Mater. Res. **8**, 233 (1993); (e) C. H. Chu and M. H. Hon, Dia. Rel. Materials **2**, 311 (1993); (f) F. C.-N. Hong, J.-C. Hsieh, J.-J. Wu, G.-T. Liang, and J.-H. Hwang, Dia. Rel. Materials **2**, 365 (1993).

5. T. I. Hukka, R. I. Rawles, and M. P. D'Evelyn, Thin Solid Films **225**, 212 (1993).

6. T. Suntola, Mater. Sci. Reports **4**, 265 (1989).

7. P. Hirva and T. A. Pakkanen, Surface Sci. **220**, 137 (1989).

8. J. Nishizawa, K. Aoki, S. Suzuki, K. Kikuchi, J. Electrochem Soc. **137**, 1898 (1990).

9. J. A. Yarmoff, D. K. Shuh, T. D. Durbin, C. W. Lo, D. A. Lapiano-Smith, F. R. McFeely, and F. J. Himpsel, J. Vac. Sci. Technol. A **10**, 2303 (1992).

10. (a) D. D. Koleske, S. M. Gates, and D. B. Beach, J. Appl. Phys. **72**, 4073 (1992); (b) S. M. Gates, D. D. Koleske, J. R. Heath, and M. Copel, Appl. Phys. Lett. **62**, 510 (1993).

11. S. Imai, T. Iizuka, O. Sugiura, M. Matsumura, Thin Solid Films **225**, 168 (1993).

12. F. G. McIntosh, P. C. Colter, and S. M. Bedair, Thin Solid Films **225**, 183 (1993).

13. (a) L. Y. Tsou, Jpn. J. Appl. Phys. **25**, 1594 (1986); (b) O. Krogh, T. Wicker, and B. Chapman, J. Vac. Sci. Technol. B **4**, 1292 (1986); (c) M.-C. Chuang and J. W. Coburn, J. Vac. Sci. Technol. A **8**, 1969 (1990).

14. A. H. Boonstra, Philips Res. Repts. Suppl. No. 3 (Philips Research Laboratories, Eindoven, The Netherlands, 1968) p. 1.

15. G. A. Bootsma and F. Meyer, Surf. Sci. **14**, 52 (1969).

16. G. A. Bootsma, Surf. Sci. **15**, 340 (1969).

17. M. Miyamura, Y. Sakisaka, M. Nishijima, and M. Onchi, Surf. Sci. **72**, 243 (1978).

18. (a) A. L. Johnson, M. M. Walczak, and T. E. Madey, Langmuir **4**, 277 (1988); (b) S. A. Joyce, J. A. Yarmoff, A. L. Johnson, and T. E. Madey, Mater. Res. Soc. Symp. Proc. **131**, 185 (1989).

19. (a) B. I. Craig and P. V. Smith, Surf. Sci. **239**, 36 (1990); (b) B.I. Craig and P.V. Smith, Surf. Sci. **262**, 235 (1992)..

20. Q. Gao, C. C. Cheng, P. J. Chen, W. J. Choyke, and J. T. Yates, Jr., Thin Solid Films **225**, 140 (1993).

21. P. A. Coon, P. Gupta, M. L. Wise, and S. M. George, J. Vac. Sci. Technol. A **10**, 324 (1992).

22. A. H. Boonstra and J. Van Ruler, Surf. Sci. **4**, 141 (1966).

23. S. M. Cohen, T. I. Hukka, Y. L. Yang, and M. P. D'Evelyn, Thin Solid Films **225**, 155 (1993). Subsequent to its publication, we discovered an error in the calibration for hydrogen coverages greater than 1 ML in Fig. 1 of this paper, which resulted from a decrease in the chamber pumping speed following the large doses necessary to produce these coverages. The corrected coverages are 1.13, 1.07, 0.96, 0.43, 0.15, and 0.07 ML. None of the conclusions of the paper are affected by this correction.

24. Y. L. Yang, S. M. Cohen, and M. P. D'Evelyn, Mater. Res. Soc. Symp. Proc. **282**, 421 (1993).

25. R. E. Thomas, R. A. Rudder, and R. J. Markunas, Mater. Res. Soc. Symp. Proc. **204**, 327 (1991).

26. C. C. Cheng, S. R. Lucas, H. Gutleben, W. J. Choke, and J. T. Yates, Jr., J. Am. Chem. Soc. **114**, 1249 (1992).

27. D. D. Koleske and S. M. Gates, J. Chem. Phys. **98**, 5091 (1993).

28. J. A. Appelbaum, G. A. Baraff, D. R. Hamann, H. D. Hagstrum, and T. Sakurai, Surface Sci. **70**, 654 (1978).

29. L. Papagno, X. Y. Shen, J. Anderson, G. S. Spagnolo, and G. J. Lapeyre, Phys. Rev. B **34**, 7188 (1986).

30. Y. J. Chabal, Surf. Sci. **168**, 594 (1986).

31. (a) H. Ibach and J. E. Rowe, Surf. Sci. **43**, 481 (1974); (b) F. Stucki, J. A. Schaefer, J. R. Anderson, G. J. Lapeyre, and W. Göpel, Solid State Commun. **47**, 795 (1983); (c) R. Butz, E. M. Oellig, H. Ibach, and H. Wagner, Surf. Sci. **147**, 343 (1984); (d) Y. J. Chabal and K. Raghavachari, Phys. Rev. Lett. **53**, 282 (1984); (e) L. S. O. Johansson, R. I. G. Uhrberg, and G. V. Hansson, Phys. Rev. B **38**, 13490 (1988); (f) J. J. Boland, Surface Sci. **261**, 17 (1992); (g) J. E. Northrup, Phys. Rev. B **44**, 1419 (1991). 2x1, 1x1, 3x1; (h) Z. Jing and J. L. Whitten, Phys. Rev. B **46**, 9544 (1992).

32. P. Nachtigall, K.D. Jordan, and K.C. Janda, J. Chem. Phys. **95**, 8652 (1991).

33. C.J. Wu and E.A. Carter, Chem. Phys. Lett. **185**, 172 (1991).

34. R.D. Schnell, F.J. Himpsel, A. Bogen, D. Rieger, and W. Steinmann, Phys. Rev. B **32**, 8052 (1985).

35. J. E. Rowe, G. Margaritondo, and S. B. Christmann, Phys. Rev. B **16**, 1581 (1977).

36. (a) P. H. Citrin, J. E. Rowe, and P. Eisenberger, Phys. Rev. B **28**, 2299 (1983); (b) G. B. Bachelet and M. Schlüter, Phys. Rev. B **28**, 2302 (1983).

37. M. J. Bedzyk and G. Materlik, Phys. Rev. B **31**, 4110 (1985).

38. (a) N. Aoto, E. Ikawa, and Y. Kurogi, Surface Sci. **199**, 408 (1988); (b) G. Thornton, P.L. Wincott, R. McGrath, I.T. McGovern, F.M. Quinn, D. Norman, and D.D. Vvedensky, Surf. Sci. **211/212**, 959 (1989); (c) L. S. O. Johansson, R. I. G. Uhrberg, R. Lindsay, P. L. Wincott, and G. Thornton, Phys. Rev. B **42**, 9534 (1990); (d) D. Purdie, C. A. Muryn, N. S. Prakesh, K. G. Purcell, P. L. Wincott, D. Norman, G. Thornton, and D. S.-L. Law, J. Phys. Condens. Matter **3**, 7751 (1991).

39. Q. Gao, C. C. Cheng, P. J. Chen, W. J. Choyke, and J. T. Yates, Jr., J. Chem. Phys. **98**, 8308 (1993).

40. J. J. Boland, Presentation at the 39th American Vacuum Society National Symposium, Chicago, IL, USA (November 1992), and to be published.

41. K. Sinniah, M. G. Sherman, L. B. Lewis, W. H. Weinberg, J. T. Yates, Jr., and K. C. Janda, J. Chem. Phys. **92**, 5700 (1990).

42. M. L. Wise, B. G. Koehler, P. Gupta, P. A. Coon, and S. M. George, Surf. Sci. **258**, 166 (1991).

43. M. P. D'Evelyn, Y. L. Yang, and L. F. Sutcu, J. Chem. Phys. **96**, 852 (1992).

44. U. Höfer, L. Li, and T. F. Heinz, Phys. Rev. B **45**, 9485 (1992).

45. M. C. Flowers, N. B. H. Jonathan, Y. Liu, and A. Morris, J. Chem. Phys. (in press).

46. M. P. D'Evelyn, S. M. Cohen, E. Rouchouze, and Y. L. Yang, J. Chem. Phys. **98**, 3560 (1993).

47. (a) B. G. Koehler, C. H. Mak, D. A. Arthur, P. A. Coon, and S. M. George, J. Chem. Phys. **89**, 1709 (1988); (b) G. A. Reider, U. Höfer, and T. F. Heinz, J. Chem. Phys. **94**, 4080 (1991).

48. L. Surnev and M. Tikhov, Surf. Sci. **138**, 40 (1984).

49. (a) R. E. Thomas, R. A. Rudder, and R. J. Markunas, J. Vac. Sci. Technol. A **10**, 2451 (1992); (b) Y. L. Yang, L. M. Struck, L. F. Sutcu, and M. P. D'Evelyn, Thin Solid Films **225**, 203 (1993).

50. K. W. Kolasinski, S. F. Shane, and R. N. Zare, J. Chem. Phys. **96**, 3995 (1992).

51. S. F. Shane, K. W. Kolasinski, and R. N. Zare, J. Chem. Phys. **97**, 3704 (1992).

52. Y.-S. Park, J.-Y. Kim, and J. Lee, J. Chem. Phys. **98** (1993) 757.

53. K. W. Kolasinski, W. Nessler, A. de Meijere, and E. Hasselbrink, submitted to Phys. Rev. Lett.

54. (a) J. J. Boland, Phys. Rev. Lett. **67**, 1539 (1991); (b) J. J. Boland, J. Vac. Sci. Technol. A **10**, 2458 (1992).

55. (a) J. A. Appelbaum, G. A. Baraff, and D. R. Hamann, Phys. Rev. B **14**, 588 (1976); (b) R. J. Hamers, Ph. Avouris, and F. Boszo, Phys. Rev. Lett. **59**, 2071 (1987).

56. Z. Jing and J. L. Whitten, J. Chem. Phys. **98**, 7466 (1993).

57. C. J. Wu, I. V. Ionova, and E. A. Carter, Surf. Sci. (in press).

58. R. B. Jackman, H. Ebert, and J.S. Foord, Surf. Sci. **176**, 183 (1986).

59. R. B. Jackman, R. J. Price, J. S. Foord, Appl. Surf. Sci. **36**, 296 (1989).

60. R. J. Madix and J. A. Schwartz, Surface Sci. **24**, 264 (1971).

61. R. J. Madix and A. A. Susu, J. Vac. Sci. Technol. **9**, 915 (1972).

62. S. M. Cohen, Y. L. Yang, E. Rouchouze, T. Jin, and M. P. D'Evelyn, J. Vac. Sci. Technol. A **10**, 2166 (1992).

63. M. P. D'Evelyn, Y. L. Yang, S. M. Cohen, and L. M. Struck, to be published.

64. S. M. Cohen and M. P. D'Evelyn, J. Vac. Sci. Technol. A **9**, 2414 (1991).

65. V. T. Smith, L. M. Struck, and M. P. D'Evelyn, unpublished results.

66. K. T. Leung, L. J. Terminello, Z. Hussain, X. S. Zhang, T. Hayashi, and D. A. Shirley, Phys. Rev. B **38**, 8241 (1988).

67. H. J. Kuhr, W. Ranke, and J. Finster, Surf. Sci. **178**, 171 (1986).

68. (a) S. M. Gates, C. M. Greenlief, and D. B. Beach, J. Chem. Phys. **93**, 7493 (1990); (b) C. C. Cheng and J. T. Yates, Jr., Phys. Rev. B **43**, 4041 (1991).

69. Y. L. Yang and M. P. D'Evelyn, J. Vac. Sci. Technol. A **11**, 2200 (1993).

70. M. P. D'Evelyn, in preparation.

71. S. M. Cohen, Ph.D. Dissertation, Department of Chemistry, Rice University, 1992 (unpublished).

72. R. West, M. J. Fink, and J. Michl, Science **214**, 1343 (1981).

73. S. Masamune, Y. Hanzawa, and D. J. Williams, J. Am. Chem. Soc. **104**, 6136 (1982).

74. (a) A. H. Cowley, Polyhedron **3**, 389 (1984); (b) J. C. Corey, in *The Chemistry of Organic Silicon Compounds*, Part 1, edited by S. Patai and Z. Rappaport (Wiley, Chichester, UK, 1989), 34; (c) G. Raabe and J. Michl, in *The Chemistry of Organic Silicon Compounds*, Part 2, edited by S. Patai and Z. Rappaport (Wiley, Chichester, UK, 1989), 1015.

75. F. Grey, R. L. Johnson, J. S. Pedersen, R. Feidenhans'l, and M. Nielsen, in *The Structure of Surfaces II* (Proc. 2nd International Conference on the Structure of Solid Surfaces), edited by J. F. van der Veen and M. A. Van Hove (Springer-Verlag, Berlin, 1988), p. 292.

76. M. Needels, M. C. Payne, and J. D. Joannopoulos, Phys. Rev. Lett. **58**, 1765 (1987).

77. (a) J. T. Snow, S. Murakami, S. Masamune, and D. J. Williams, Tetrahed. Lett. **25**, 4191 (1984); (b) P. B. Hitchcock, M. F. Lapper, S. J. Miles, and A. J. Thorne, J. Chem. Soc. Chem. Commun. (1984), 480; (c) S. A. Batcheller, T. Tsumuraya, O. Tempkin, W. M. Davis, and S. Masamune, J. Am. Chem. Soc. **112**, 9394 (1990).

78. (a) J. Y. Corey and R. West, J. Am. Chem. Soc. **85**, 2430 (1963); (b) R. E. Dessy and W. Kitching, Adv. Organomet. Chem. **4**, 268 (1984); (c) F. A. Carey and C.-L. W. Hsu, J. Organomet. Chem. **19**, 29 (1969); (d) S. Nagase and T. Kudo, Organomet. **3**, 324 (1984); (e) J. Chojnowski and W. Stanczyk, Adv. Organomet. Chem. **30**, 243 (1990).

79. S. Nagase, T. Kudo, and K. Ito, in *Applied Quantum Chemistry*, edited by V. H. Smith, Jr., H. F. Schaefer III, and M. Morokuma (D. Reidel, Dordrecht, 1986) p. 249.

80. C.U.S. Larsson and A.S. Flodström, Phys. Rev. B **43**, 9281 (1991).

81. P. Kisliuk, J. Phys. Chem. Solids **3**, 95 (1957) and **5**, 78 (1958).

82. For example, K. Laidler, *Chemical Kinetics*, 3rd Edition (Harper & Row, New York, 1987).

83. K. P. Huber and G. Herzberg, *Molecular Spectra and Molecular Structure, Vol. IV, Constants of Diatomic Molecules* (Van Nostrand, New York, 1979). The vibrational frequency of HBr

is 11% less than that of HCl, corresponding to a 20% smaller force constant, taking the reduced masses into account.

84. L. Andersohn and U. Köhler, Surf. Sci. **284**, 77 (1993).

85. M. Chander, Y. Z. Li, J. C. Patrin, and J. H. Weaver, Phys. Rev. B (in press).

86. (a) R. M. Tromp, R. J. Hamers, and J. E. Demuth, Phys. Rev. B **34**, 5343 (1984); (b) R. J. Hamers and U. K. Köhler, J. Vac. Sci. Technol. A **7**, 2854 (1989).

87. (a) H.J. Kuhr and W. Ranke, Surf. Sci. **187**, 98 (1987); (b) H.J. Kuhr and W. Ranke, Surf. Sci. **189/90**, 420 (1987).

88. W. Ranke and Y. R. Xing, Surf. Sci. **157**, 339 (1985).

89. E. Schröder-Bergen and W. Ranke, Surf. Sci. **236**, 103 (1990).

90. M. J. Dresser, P. A. Taylor, R. M. Wallace, W. J. Choyke, and J. T. Yates, Jr., Surf. Sci. **218**, 75 (1989).

91. C. C. Cheng, R. M. Wallace, P. A. Taylor, W. J. Choyke, and J. T. Yates, Jr., J. Appl. Phys. **67**, 3693 (1990).

92. J. J. Boland, private communication to MPD.

93. (a) Y. J. Chabal, J. Vac. Sci. Technol. A **3**, 1448 (1985); (b) C. U. S. Larsson, A. L. Johnson, A. Flodström, and T. E. Madey, J. Vac. Sci. Technol. A **5**, 842 (1987).

94. J. Yoshinobu, H. Tsuda, M. Onchi, and M. Nishijima, J. Chem. Phys. **87**, 7332 (1987).

95. M. Nishijima, J. Yoshinobu, H. Tsuda, and M. Onchi, Surf. Sci. **192**, 383 (1987).

96. S. Tanaka, M. Onchi, and M. Nishijima, J. Chem. Phys. **91**, 2712 (1989).

97. (a) P. N. Noble and R. Walsh, Int. J. Chem. Kin. **15**, 547 (1983); (b) B. Ruscic, M. Schwartz, and J. Berkowitz, J. Chem. Phys. **92**, 1865 (1990).

98. J. M. Kanabus-Kaminska, J. A. Hawari, D. Griller, and C. Chatgilialoglu, J. Am. Chem. Soc. **109**, 5267 (1987).

99. R. Walsh, Acc. Chem. Res. **14**, 246 (1981).

100. F. Glockling, *The Chemistry of Germanium* (Academic Press, London, 1969) p. 10.

101. M. W. Chase, Jr., C. A. Davies, J. R. Downey, Jr., D. J. Frurip, R. A. McDonald, and A. N. Syverud, JANAF Thermochemical Tables, 3rd Ed., J. Phys. Chem. Ref. Data **14**, Supplement No. 1 (1985).

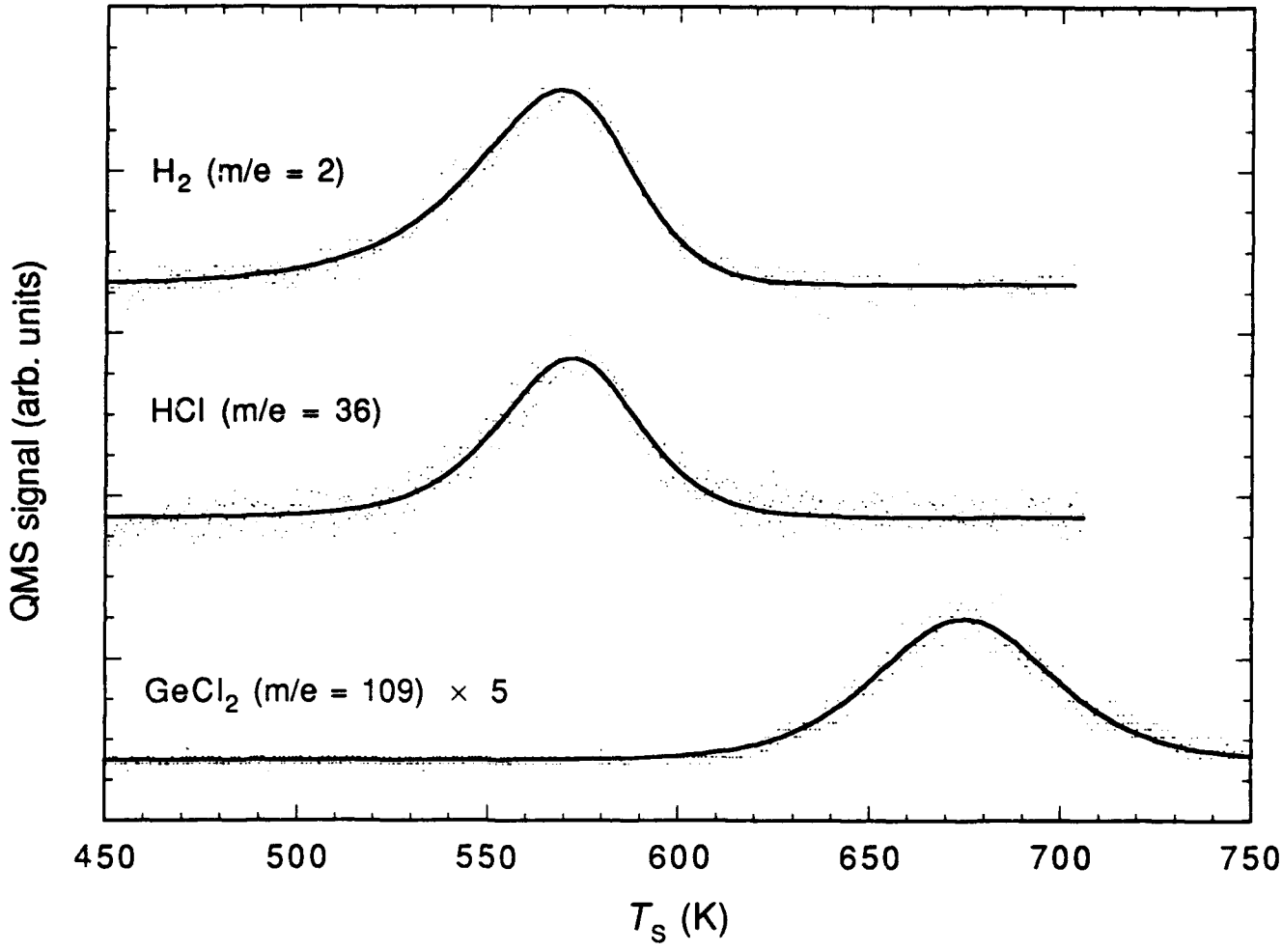

Fig. 1. TPD spectrum of desorption products from Ge(100) following a saturation dose of HCl. For $GeCl_2$ the $GeCl^+$ cracking fraction was actually detected.

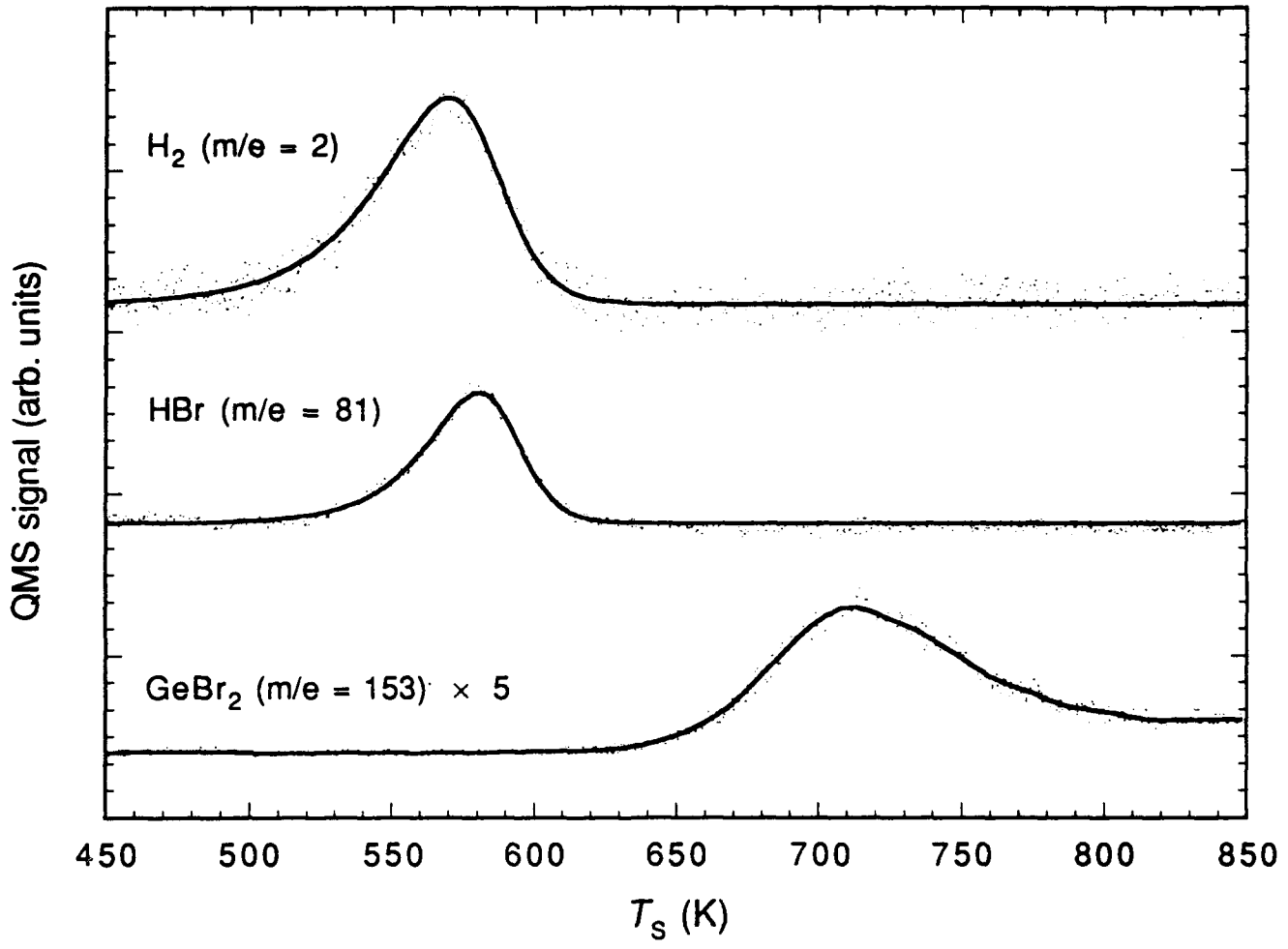

Fig. 2. TPD spectrum of desorption products from Ge(100) following a saturation dose of HBr. For $GeBr_2$ the $GeBr^+$ cracking fraction was actually detected.

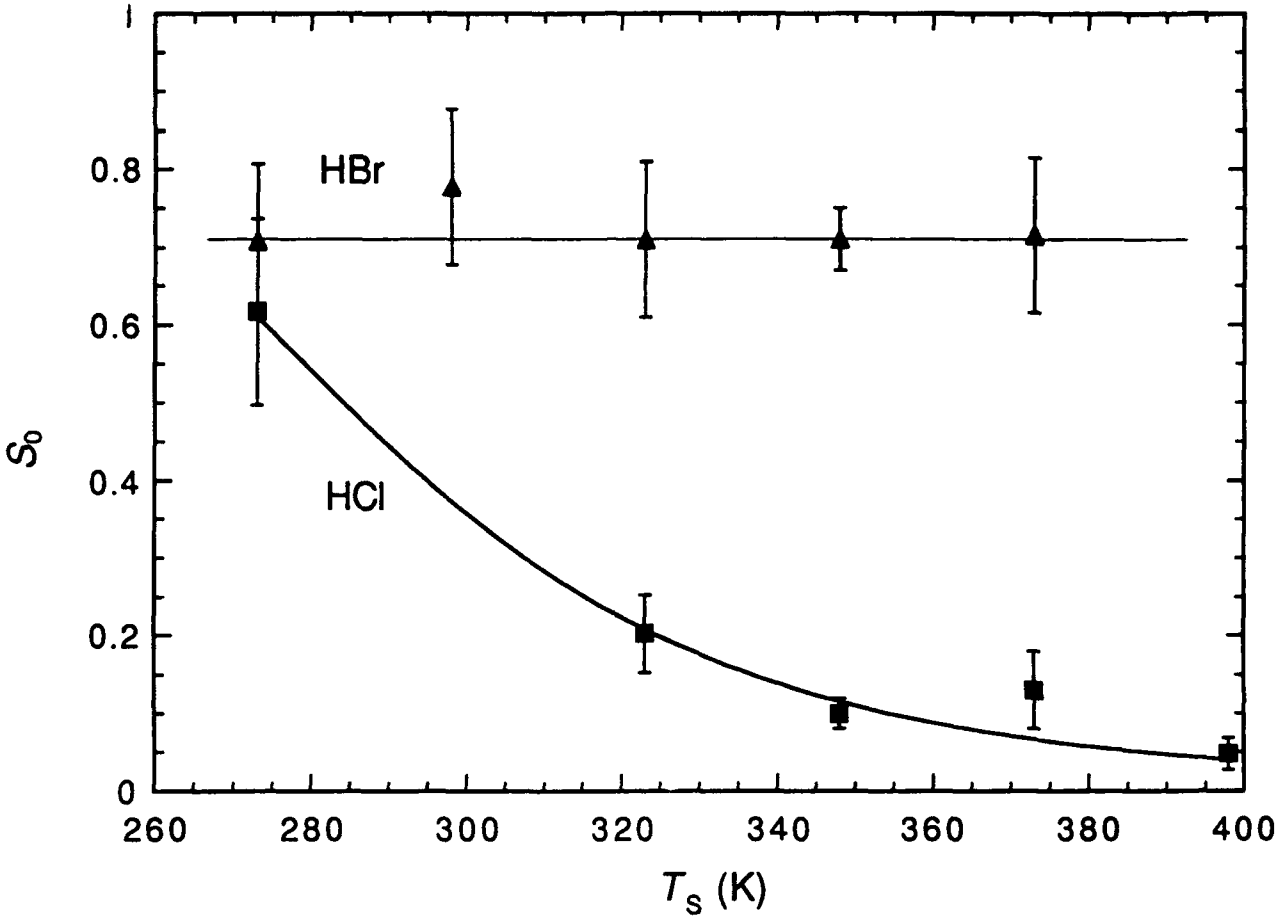

Fig. 3. Surface temperature dependence of initial sticking probability, S_0, of HCl and HBr on Ge(100). Curve through HCl data: fit to predictions of precursor model (Eq. (13)) with $\alpha = 1$, $\nu_d/\nu_c = 7 \times 10^4$, and E_d-E_c = 6.3 kcal/mol.

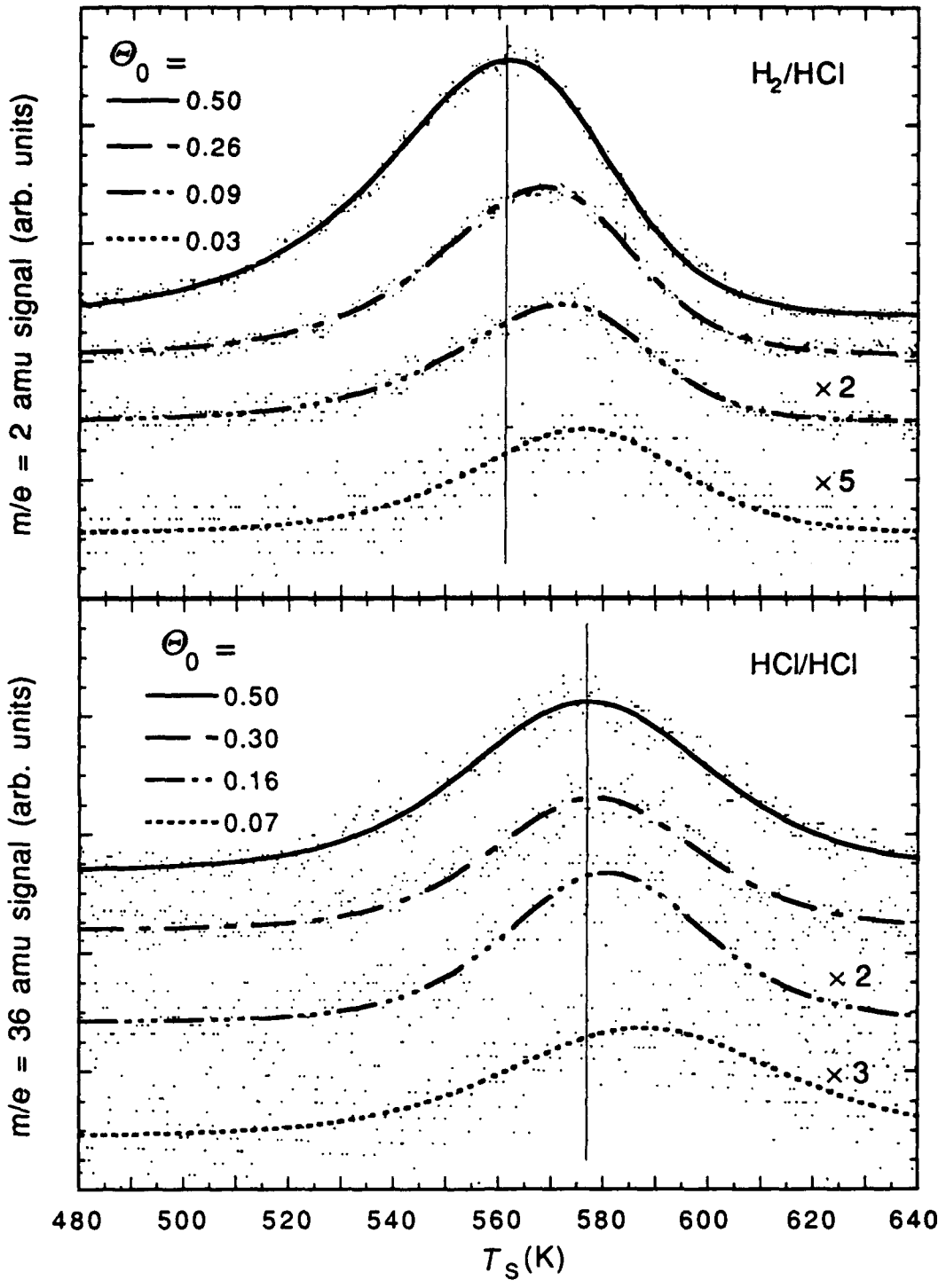

Fig. 4. TPD spectra (2 K s^{-1} heating rate) of H_2 and HCl desorption products from Ge(100) following various doses of HCl. The initial HCl coverage is indicated for each trace.

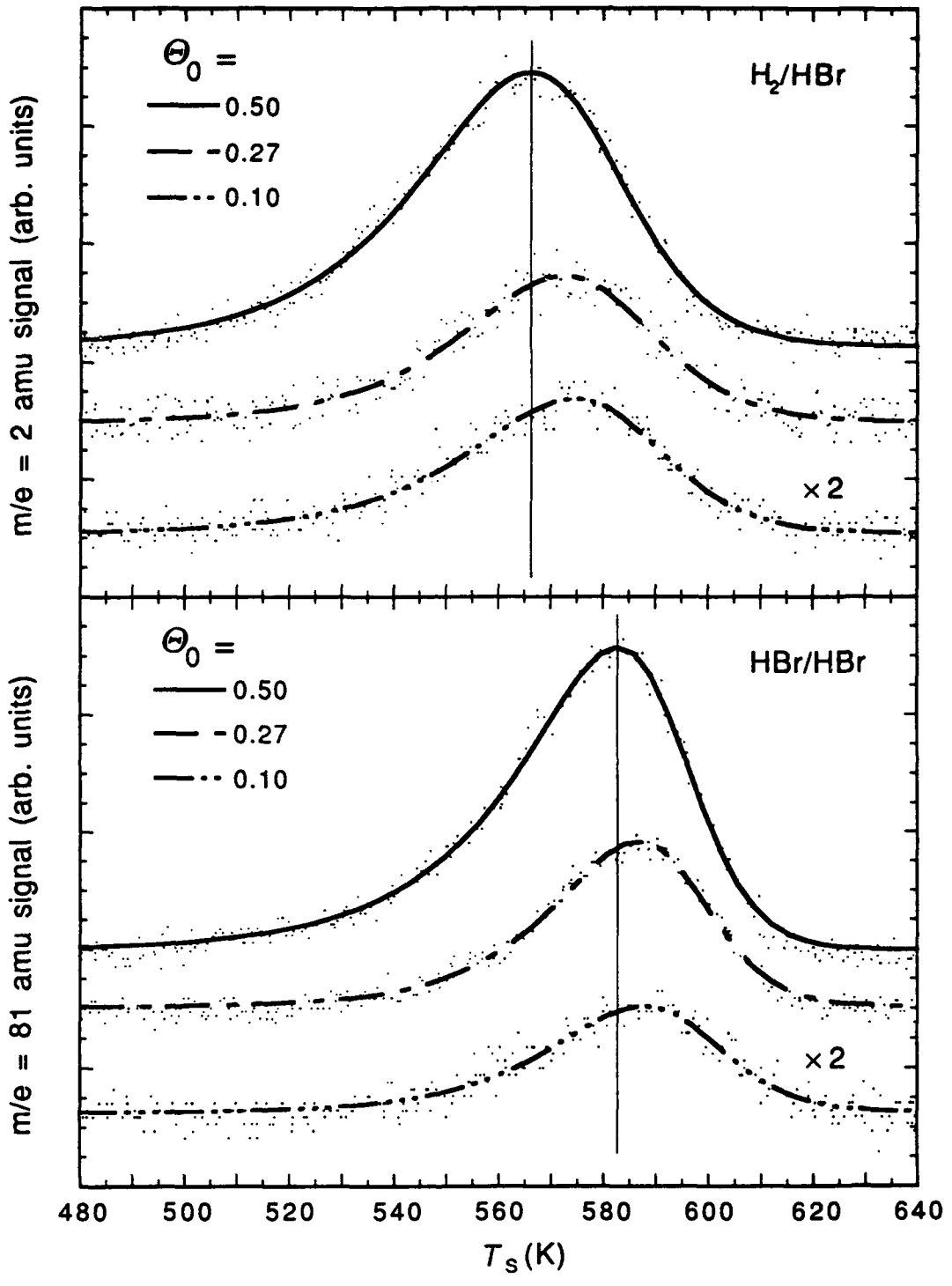

Fig. 5. TPD spectra (2 K s^{-1} heating rate) of H_2 and HBr desorption products from Ge(100) following various doses of HBr. The initial HBr coverage is indicated for each trace.

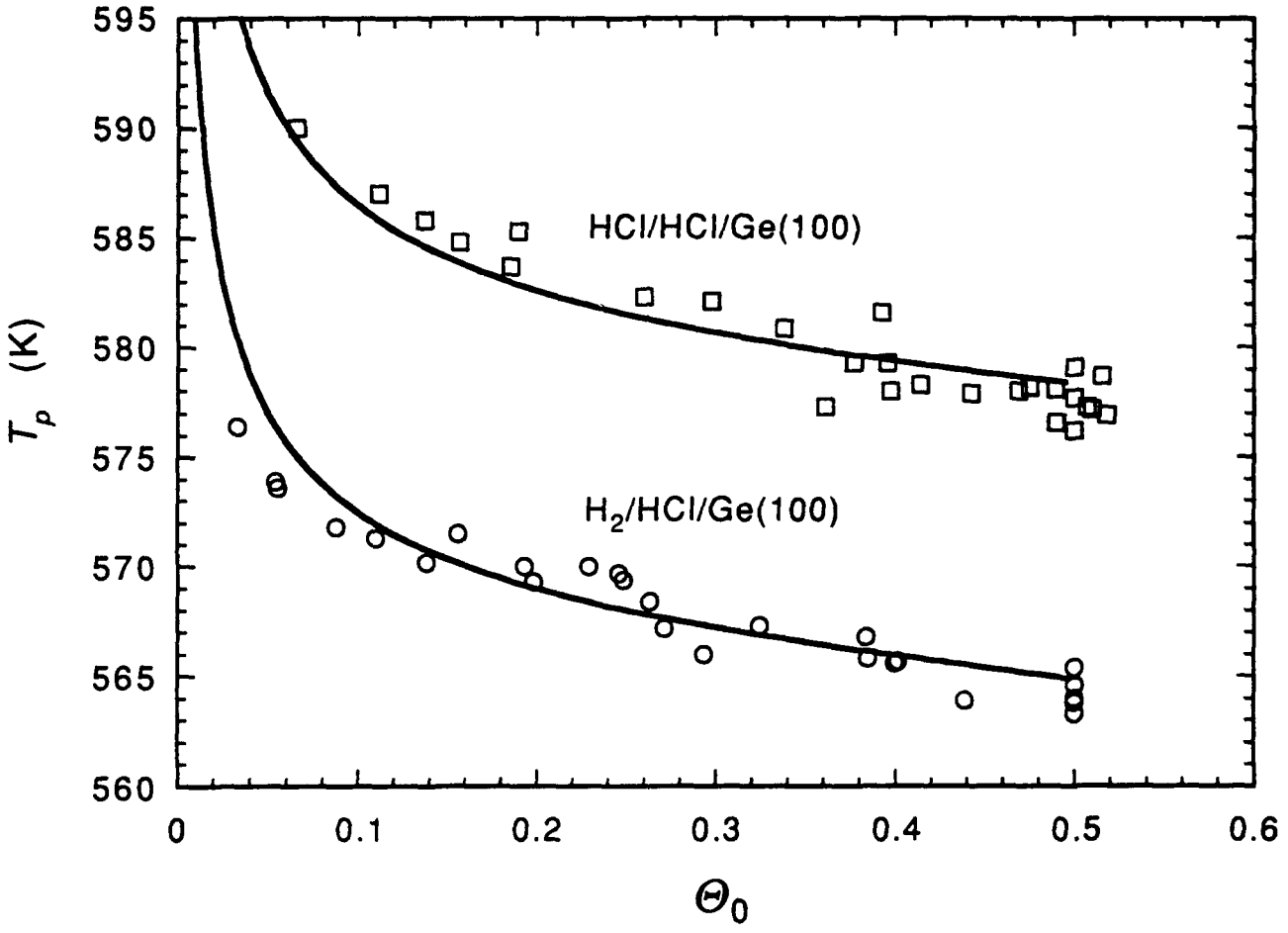

Fig. 6. Dependence of TPD peak temperatures for H_2 and HCl on initial coverage of HCl. Curves through data: prediction of competitive pairing model with $\varepsilon_{HH} = \varepsilon_{HCl} = \varepsilon_{ClCl} =$ 2.7 kcal/mol, and $E_{a,HH}$, $E_{a,HCl}$ = 41.4 and 38.1 kcal/mol, respectively.

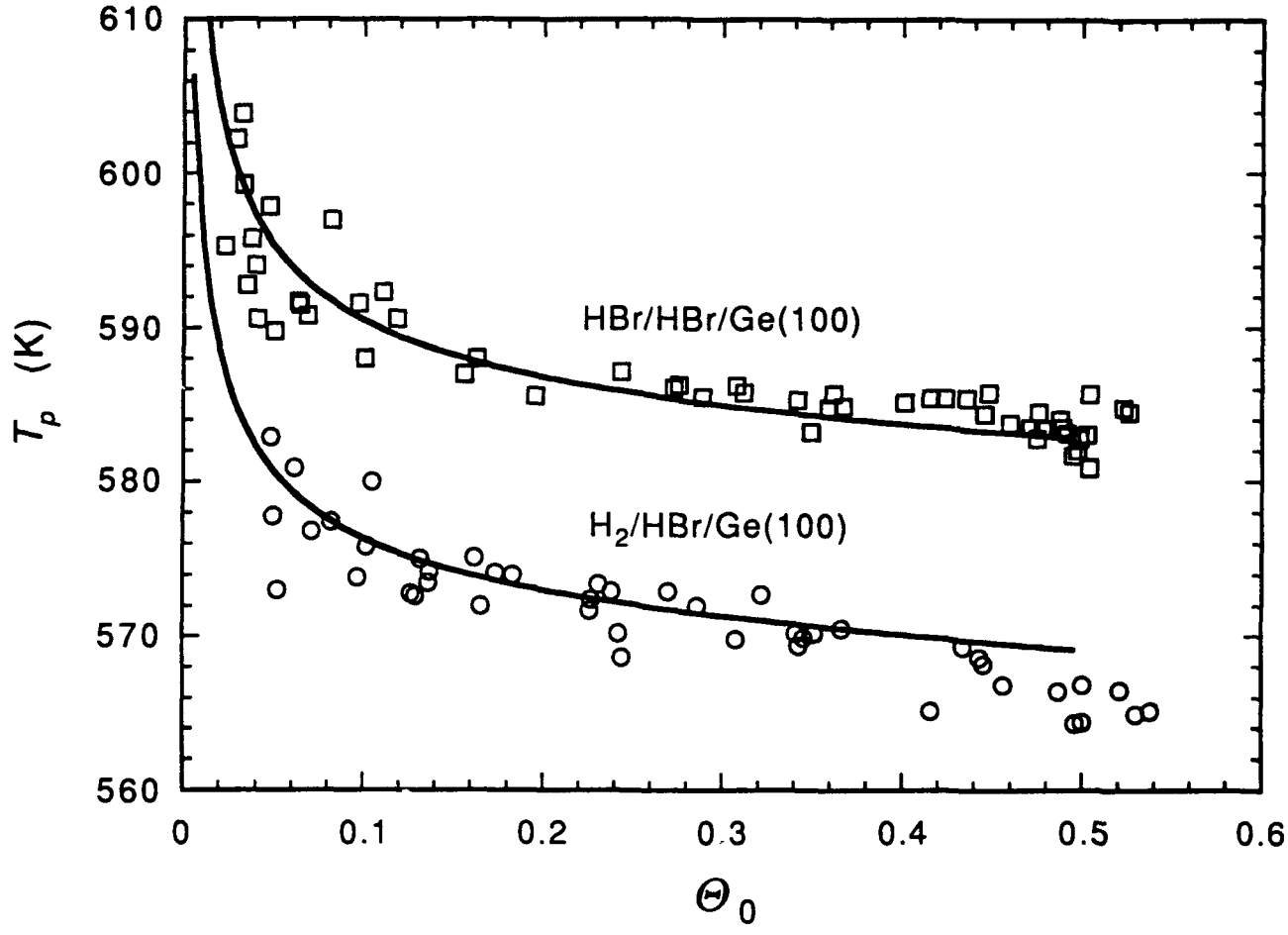

Fig. 7. Dependence of TPD peak temperatures for H_2 and HBr on initial coverage of HBr. Curves through data: prediction of competitive pairing model with $\varepsilon_{HH} = \varepsilon_{HBr} = \varepsilon_{BrBr}$ = 2.8 kcal/mol, and $E_{a,HH}$, $E_{a,HBr}$ = 41.7 and 38.5 kcal/mol, respectively.

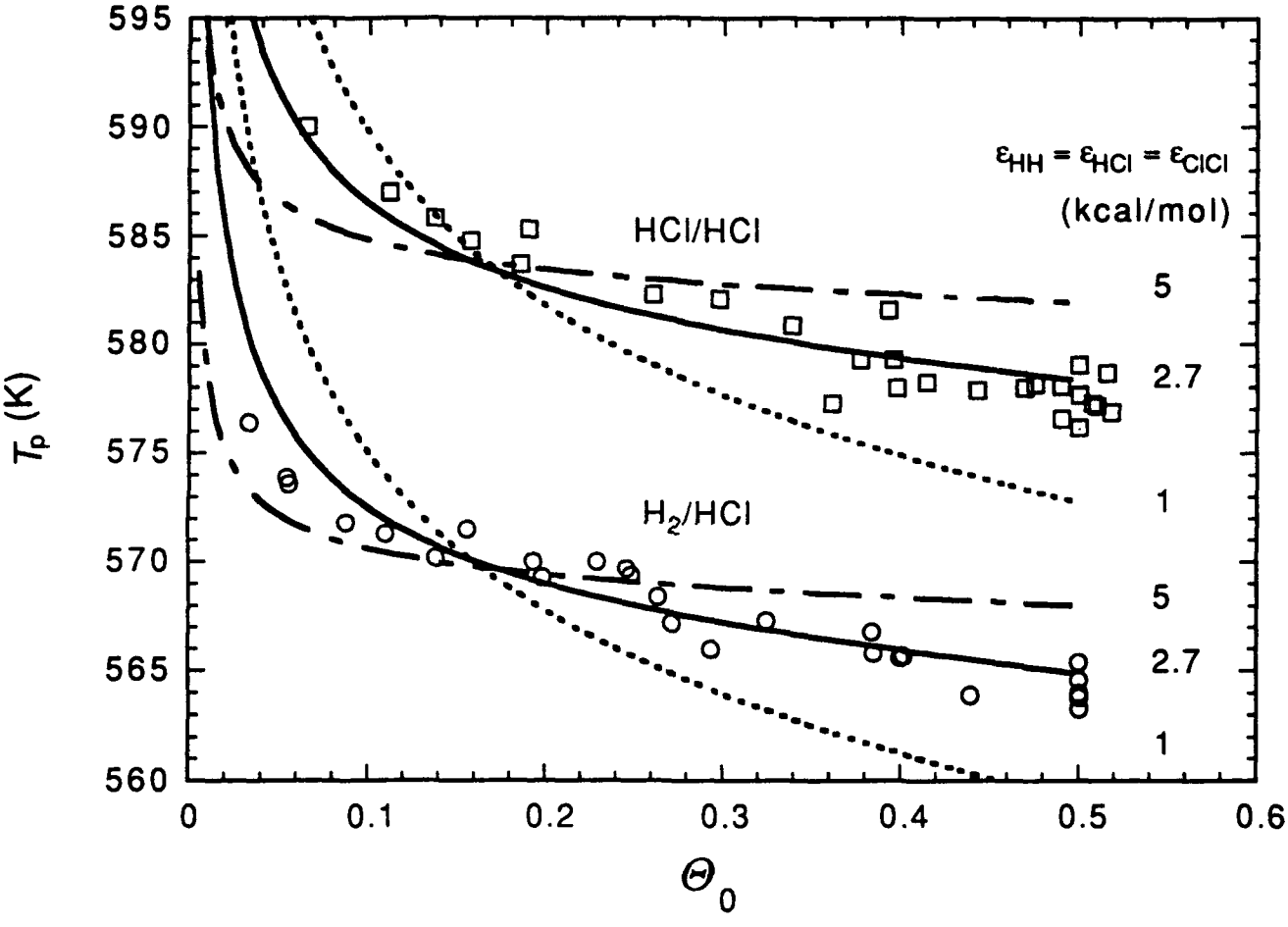

Fig. 8. Predictions of competitive pairing model with various values of $\varepsilon_{HH} = \varepsilon_{HCl} = \varepsilon_{ClCl} = \varepsilon$, compared with experimental data for HCl. For ε = 5, 2.7, and 1 kcal/mol $E_{a,HH}$ was 41.7, 41.4, and 41.0 kcal/mol, and $E_{a,HCl}$ was 38.6, 38.1, and 37.7 kcal/mol, respectively. The latter values were adjusted slightly in each case to best reproduce the TPD peak temperatures and relative yields of H_2 and HCl.

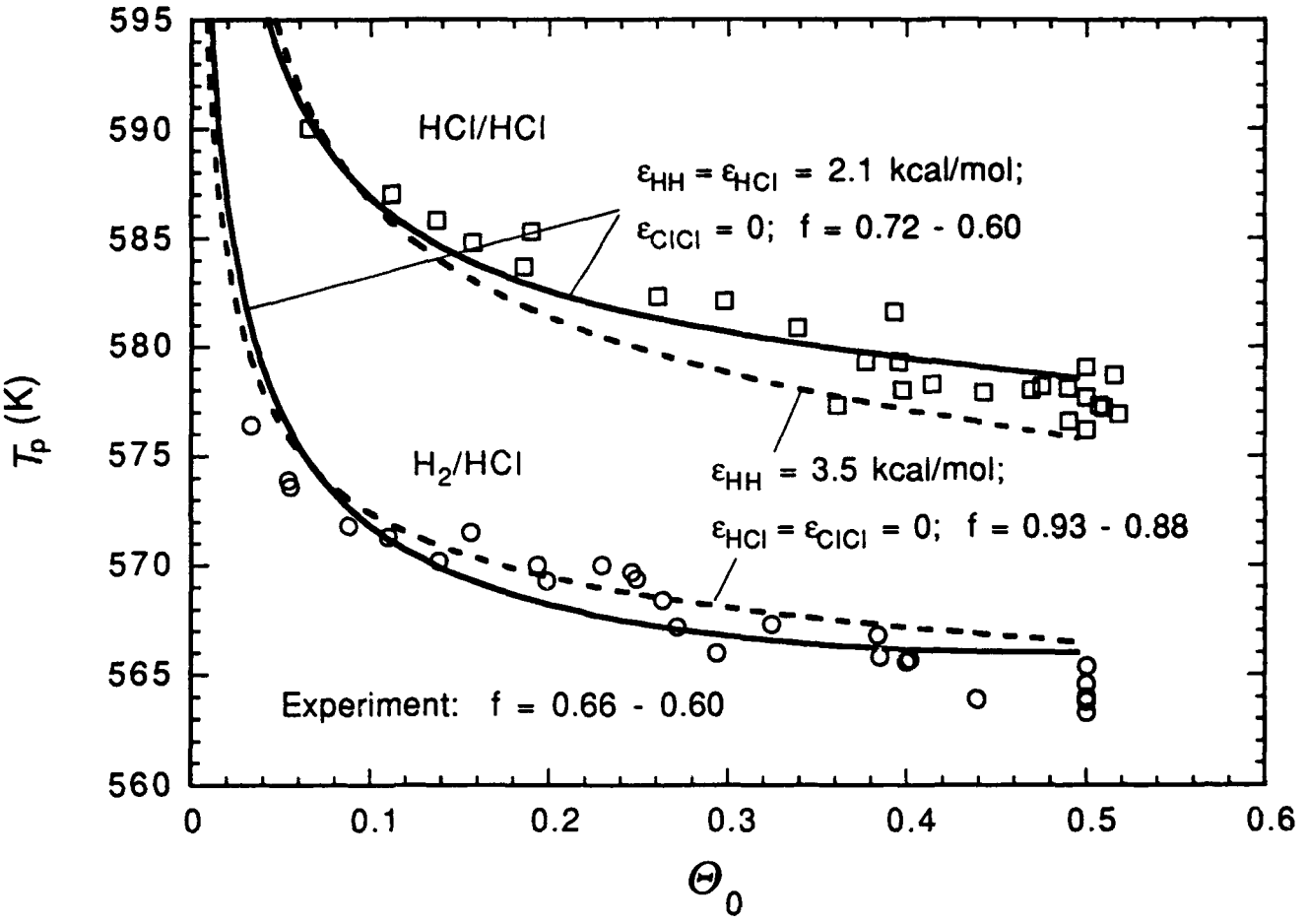

Fig. 9. Predictions of competitive pairing model with different assumed pairing energies compared with experimental data for HCl. Dashed curves: ε_{HH} = 3.5 kcal/mol, ε_{HCl} = ε_{ClCl}= 0, $E_{a,HH}$ = 41.9 kcal/mol, $E_{a,HCl}$ = 37.9 kcal/mol. Solid curves: ε_{HH} = ε_{HCl} = 2.1 kcal/mol, ε_{ClCl}= 0, $E_{a,HH}$ = 41.1 kcal/mol, $E_{a,HCl}$ = 38.3 kcal/mol. The range of predicted values of f, the fraction of hydrogen desorbing as H_2, over the initial coverage range of 0.05 - 0.5 ML is given in each case.

TECHNICAL REPORT DISTRIBUTION LIST - GENERAL

Office of Naval Research (1)*
Chemistry Division, Code 313
800 North Quincy Street
Arlington, Virginia 22217-5000

Defense Technical Information Center (2)
Building 5, Cameron Station
Alexandria, VA 22314

Dr. James S. Murday (1)
Chemistry Division, Code 6100
Naval Research Laboratory
Washington, D.C. 20375-5000

Dr. Robert Green, Director (1)
Chemistry Division, Code 385
Naval Air Weapons Center
Weapons Division
China Lake, CA 93555-6001

Dr. Elek Lindner (1)
Naval Command, Control and
Ocean Surveillance Center
RDT&E Division
San Diego, CA 92152-5000

Dr. Richard W. Drisko (1)
Naval Civil Engineering
Laboratory
Code L52
Port Hueneme, CA 93043

Dr. Harold H. Singerman (1)
Naval Surface Warfare Center
Carderock Division Detachment
Annapolis, MD 21402-1198

Dr. Eugene C. Fischer (1)
Code 2840
Naval Surface Warfare Center
Carderock Division Detachment
Annapolis, MD 21402-1198

Dr. Bernard E. Douda (1)
Crane Division
Naval Surface Warfare Center
Crane, Indiana 47522-5000

* Number of copies to forward